

A fast implicit difference scheme for solving the generalized time-space fractional diffusion equations with variable coefficients

Xian-Ming Gu^{a,b}, Ting-Zhu Huang^{c,*}, Yong-Liang Zhao^c, Pin Lyu^a, Bruno Carpentieri^d

^a*School of Economic Mathematics/Institute of Mathematics,
Southwestern University of Finance and Economics, Chengdu 611130, Sichuan, P.R. China*

^b*Bernoulli Institute of Mathematics, Computer Science and Artificial Intelligence,
University of Groningen, Nijenborgh 9, P.O. Box 407, 9700 AK Groningen, The Netherlands*

^c*School of Mathematical Sciences,
University of Electronic Science and Technology of China, Chengdu, Sichuan 611731, P.R. China*

^d*Facoltà di Scienze e Tecnologie informatiche,
Libera Università di Bolzano, Dominikanerplatz 3 - piazza Domenicani, 3 Italy - 39100, Bozen-Bolzano*

Abstract

In this paper, we first propose an unconditionally stable implicit difference scheme for solving generalized time-space fractional diffusion equations (GTSFDEs) with variable coefficients. The numerical scheme utilizes the $L1$ -type formula for the generalized Caputo fractional derivative in time discretization and the second-order weighted and shifted Grünwald difference (WSGD) formula in spatial discretization, respectively. Theoretical results and numerical tests are conducted to verify the $(2 - \gamma)$ -order and 2-order of temporal and spatial convergence with $\gamma \in (0, 1]$ the order of Caputo fractional derivative, respectively. The fast sum-of-exponential approximation of the generalized Caputo fractional derivative and Toeplitz-like coefficient matrices are also developed to accelerate the proposed implicit difference scheme. Numerical experiments show the effectiveness of the proposed numerical scheme and its good potential for large-scale simulation of GTSFDEs.

Keywords: Implicit difference scheme, GTSFDEs, Generalized Caputo fractional derivative, WSGD, Fast Fourier transform, Krylov subspace method.

1. Introduction

In recent years there has been a growing interest in the field of fractional calculus. For instance, Podlubny [1], Samko *et al.* [2] and Kilbas *et al.* [3] provide the history and a comprehensive treatment of this subject. Many phenomena in engineering, physics, chemistry and other sciences can be described very successfully by using fractional partial differential equations (FPDEs). Diffusion with an additional velocity field and diffusion under the influence of a constant external force field are, in the Brownian case, both modelled by the diffusion equation. In the case of anomalous diffusion this is no longer true, i.e., the space fractional generalization may be different for the transport in external force field [4]. Under the framework of the continuous time random walks (CTRWs) model, the fractional diffusion, Fokker-Planck and Feynman-Kac equations [4, 5] can be derived with power-law waiting time distribution (WTD), assuming the particles may exhibit long waiting time. However, for some practical physical processes, it is necessary to make the first moment of the waiting time measure finite. This leads to the generalized time fractional diffusion equation corresponding to the CTRWs model with some more complicated WTDs (beyond the power-law limit) [6–8], e.g., the tempered [9–13] and the scale-weight [14, 15] power law WTDs. In one word, the generalization

*Corresponding author

Email addresses: guxianming@live.cn, guxm@swufe.edu.cn (Xian-Ming Gu), tingzhu Huang@126.com (Ting-Zhu Huang), ylzhaofde@sina.com (Yong-Liang Zhao), plyu@swufe.edu.cn (Pin Lyu), bcarpentieri@gmail.com (Bruno Carpentieri)

of time-space fractional diffusion equations where the sub-diffusion in time and the super-diffusion in space simultaneously [16] will be meaningful to model the anomalous diffusion with complicated physical processes.

Based on the above considerations, in this work, we are interested in developing fast numerical methods for solving the initial-boundary value problem of the generalized time-space fractional diffusion equation (GTSFDE) with variable coefficients

$$\begin{cases} {}_0^C D_t^{\gamma, \lambda(t)} u(x, t) = \xi(x, t) \left[p_a D_x^\alpha u(x, t) + (1 - p)_x D_b^\alpha u(x, t) \right] + f(x, t), & (x, t) \in (a, b) \times (0, T), \\ u(x, 0) = \phi(x), & x \in [a, b], \\ u(a, t) = \varphi(t), \quad (b, t) = \psi(t), & t \in (0, T], \end{cases} \quad (1.1)$$

where $\alpha \in (1, 2]$, $\gamma \in (0, 1)$ and $p \in [0, 1]$. The function $u(x, t)$ can be interpreted as representing the concentration of a particle plume undergoing anomalous diffusion. The diffusion coefficient depended on both time and space variables satisfies the condition $0 < \xi_{\min} \leq \xi(x, t) < +\infty$, $\forall (x, t) \in (a, b) \times (0, t]$, and the forcing function $f(x, t)$ represents the source or sink term. In the current study, we assume that the problem (1.1) has an unique and sufficiently smooth solution [7, 8, 17, 18].

The GTSFDE (1.1) can be regarded as a generalization of classical diffusion equations where the first-order time derivative is replaced by the generalized Caputo fractional derivative of order $\gamma \in (0, 1]$ with weighting function $\lambda(t) \in C^2[0, T]$, where $\lambda(t) > 0$ and $\lambda'(t) \leq 0$ for all $t \in [0, T]$, and the second-order spatial derivative is replaced by the two-sided Riemann-Liouville (R-L) fractional derivative of order $\alpha \in (1, 2]$. Specifically, the time fractional derivative in Eq. (1.1) is the generalized Caputo fractional derivative of order γ [8] denoted by

$${}_0^C D_t^{\gamma, \lambda(t)} u(x, t) = \frac{1}{\Gamma(1 - \gamma)} \int_0^t \frac{\lambda(t - \eta)}{(t - \eta)^\gamma} \frac{\partial u(x, \eta)}{\partial \eta} d\eta, \quad (1.2)$$

which reduces to the Caputo fractional derivative when $\lambda(t) \equiv 1$. Meanwhile, the left-handed (${}_a D_x^\alpha$) and the right-handed (${}_x D_b^\alpha$) space fractional derivatives in Eq. (1.1) are the R-L fractional derivatives of order α [1] which are defined as

$${}_a D_x^\alpha u(x, t) = \frac{1}{\Gamma(2 - \alpha)} \frac{\partial^2}{\partial x^2} \int_a^x \frac{u(\xi, t) d\xi}{(x - \xi)^{\alpha-1}} \quad \text{and} \quad {}_x D_b^\alpha u(x, t) = \frac{1}{\Gamma(2 - \alpha)} \frac{\partial^2}{\partial x^2} \int_x^b \frac{u(\xi, t) d\xi}{(\xi - x)^{\alpha-1}}, \quad (1.3)$$

where $\Gamma(\cdot)$ denotes the Gamma function. Note that the above equation reduces to the classical diffusion equation for $\gamma = \lambda(t) \equiv 1$ and $\alpha = 2$.

Generally speaking, although the (semi-)analytical (or closed-form) solutions of particular (generalized) space-time fractional partial differential equations (PDEs) on the entire real line are accessible via the Laplace or Fourier transforms, yet these solutions are expressed in terms of special functions which are usually difficult for the numerical evaluation in practice. Moreover, if we define the problem (1.1) on a bounded domain, one cannot obtain any known equations for its fundamental solution; refer to [19, 20]. These naturally promote the rapid development of numerical methods for fractional PDEs. Therefore, the current study will focus on developing the numerical approaches for solving the problem (1.1).

If $\gamma = \lambda(t) \equiv 1$, the problem (1.1) collapses to the space fractional diffusion equation (SFDE) with variable coefficients. For such SFDEs, various robust numerical schemes are proposed by exploiting the shifted Grünwald discretization and the implicit Euler (or Crank-Nicolson) time-stepping procedure for two-sided R-L fractional derivatives and the first-order time derivative, respectively; refer to [21–23] for details. To improve the convergence order of such numerical methods, several studies combined different second-order accurate approximations for discretizing two-sided R-L fractional derivatives with the Crank-Nicolson technique in order to obtain the second-order finite difference schemes for solving the SFDEs with variable coefficients. However, the unconditional convergence of such second-order finite difference schemes is not easy to prove, refer to [24–32] for discussions of this issue. However, these studies verified the unconditional convergence of second-order finite difference schemes often restrict diffusion coefficients positively bounded and relied on the spatial variable x . Besides, other numerical treatments including the Chebyshev-tau, finite

volume and finite element methods are proposed to solve the SFDEs with variable coefficients, refer, e.g., to [33–40] for detail.

When $\alpha = 2$, the problem (1.1) is equivalent to the generalized time fractional diffusion equation (GTFDE) with variable coefficients. Such GTFDEs were first derived and studied by Sandev *et al.* in [7]. Later, Alikhanov adopted the classical $L1$ formula [1] and employed the second-order weighted-shifted Grünwald difference (WSGD) formula [41] to approximate the generalized Caputo fractional derivative and the spatial R-L fractional derivative respectively for solving such GTFDEs with variable coefficients. Moreover, the convergence of his implicit difference schemes is proved to be unconditionally stable, refer to [8] for details. In addition, Khibie [42] has extended Alikhanov’s work to establish the stable implicit difference scheme for solving the multi-term GTFDE with variable coefficients.

On the other hand, although there are several numerical schemes about solving TSFDEs with variable coefficients –cf. $\lambda(t) \equiv 1$, however, only several difference schemes [16, 43–46] are proved to be unconditionally convergent with only first- and $(2 - \gamma)$ -order accuracy in space and time directions, respectively. It means that how to prove the unconditional convergence of implicit difference schemes with high-order spatial discretizations is often very challenging. Moreover, there are few results on numerical solutions of GTSFDEs with variable coefficients via finite difference methods in the literature. Such GTSFDEs can be regarded as a generalization of GTFDEs introduced in [7, 8] and its numerical solutions should be more difficult due to lots of computational cost arising from the nonlocal properties in both spatial and temporal fractional derivatives. Therefore, establishing an unconditionally stable numerical scheme with low computational cost for solving such GTSFDEs with variable coefficients is a promising topic and also the main motivation of our current study. In this paper, we develop the implicit difference schemes for GTSFDEs with variable coefficients, then the implicit schemes are strictly proved to be unconditionally stable and convergent with second- and $(2 - \gamma)$ -order accuracy in space and time directions, respectively. Moreover, the implicit difference schemes lead to the solutions of the resultant linear systems with Toeplitz-like coefficient matrices which can be solved via direct method in the $\mathcal{O}(N^3)$ operations along with storage $\mathcal{O}(N^2)$. However, the efficient preconditioned Krylov subspace solvers are employed to reduce the above computational and memory cost to $\mathcal{O}(N \log N)$ and $\mathcal{O}(N)$, respectively, where N is the number of spatial grid nodes. Furthermore, the fast sum-of-exponential (SOE) approximation [47] is extended to reduce computational and memory cost arising from the nonlocal property in the generalized Caputo fractional derivative with special function $\lambda(t)$ ’s. To the best of our knowledge, this is the first successful attempt to derive such a fast and stable numerical scheme of GTSFDEs with variable coefficients. Meanwhile, numerical experiments are reported to support our theoretical finding and effectiveness of the proposed schemes.

The rest of this paper is organized as follows. In Section 2, the approximations of the generalized Caputo and R-L fractional derivatives are recalled to establish the implicit difference scheme. Meanwhile, the stability and convergence of the proposed difference scheme are proved in details. In Section 3, the practical implementation of the proposed schemes is to solve a sequence of linear systems with Toeplitz-like coefficient matrices. The efficient preconditioned Krylov subspace solvers are adopted and investigated to handle such Toeplitz-like resultant linear systems. In Section 4, numerical experiments are reported to demonstrate the efficiency of the proposed method. Some concluding remarks are given in Section 5.

2. An implicit difference scheme for GTSFDEs

In this section, we first review the approximation of the generalized Caputo fractional derivative and employ the second-order WSGD approximation [41] for yielding the implicit difference scheme to the problem (1.1). Moreover, both the stability and convergence of the proposed implicit difference scheme are investigated in details.

2.1. The approximation for the generalized Caputo fractional derivative

We first briefly recall the generalized $L1$ formula for approximating the temporal fractional derivative ${}_0^C D_t^{\gamma, \lambda(t)}$ proposed in [8] and denote its approximation result by $\Delta_{0,t}^{\gamma, \lambda(t)}$. To derive the difference scheme, we first introduce a rectangle $\bar{Q}_T = \{(x, t) : a \leq x \leq b, 0 \leq t \leq T\}$ discretized on the mesh $\varpi_{h,\tau} = \varpi_h \times \varpi_\tau$,

where $\varpi_h = \{x_i = a + ih, 0 \leq i \leq N, h = \frac{b-a}{N}\}$ and $\varpi_\tau = \{t_j = j\tau, j = 0, 1, \dots, M, \tau = \frac{T}{M}\}$. We also denote by $\mathbf{v} = \{v_i \mid i = 0, 1, \dots, N\}$ any grid function. Moreover, we denote the linear interpolation over the time interval (t_j, t_{j+1}) with $0 \leq j \leq M-1$ by

$$\Pi_{1,s}v(t) = v(t_{s+1})\frac{t-t_s}{\tau} + v(t_s)\frac{t_{s+1}-t}{\tau}.$$

At each time step t_{j+1} with $j = 0, 1, \dots, M-1$, the generalized $L1$ formula is defined by

$$\begin{aligned} {}^C D_t^{\gamma, \lambda(t)} v(t)|_{t=t_{j+1}} &= \frac{1}{\Gamma(1-\gamma)} \int_0^{t_{j+1}} \frac{\lambda(t_{j+1}-\eta)v'(\eta)d\eta}{(t_{j+1}-\eta)^\gamma} \\ &= \frac{1}{\Gamma(1-\gamma)} \left(\sum_{s=0}^j v_{t,s} \int_{t_s}^{t_{s+1}} \frac{\lambda(t_{j+1}-\eta)d\eta}{(t_{j+1}-\eta)^\gamma} + \sum_{s=0}^j \int_{t_s}^{t_{s+1}} \frac{\lambda(t_{j+1}-\eta)[v(\eta) - \Pi_{1,s}v(\eta)]'d\eta}{(t_{j+1}-\eta)^\gamma} \right) \\ &= \frac{\tau^{1-\gamma}}{\Gamma(2-\gamma)} \sum_{s=0}^j [\lambda_{j-s+1/2}a_{j-s} + (\lambda_{j-s} - \lambda_{j-s+1})b_{j-s}]v_{t,s} + R_1^j + R_2^j, \end{aligned}$$

where $\lambda_s = \lambda(t_s)$ and

$$v_{t,s} = \frac{v(t_{s+1}) - v(t_s)}{\tau}, \quad a_\ell = (\ell+1)^{1-\gamma} - \ell^{1-\gamma}, \quad b_\ell = \frac{1}{2-\gamma} [(\ell+1)^{2-\gamma} - \ell^{2-\gamma}] - \frac{1}{2} [(\ell+1)^{1-\gamma} + \ell^{1-\gamma}], \quad \ell \geq 1,$$

and the definition of R_1^j , R_2^j and their estimations can be separately found in [8]. The truncation error and property of the generalized $L1$ formula are also analyzed in [8, Lemma 4.1] as follows

Lemma 2.1. Assume that $\gamma \in (0, 1)$, $\lambda(t) > 0$, $\lambda'(t) \leq 0$, and $\lambda(t), v(t) \in \mathcal{C}^2[0, t_{j+1}]$. Then

$${}^C D_t^{\gamma, \lambda(t)} v(t_{j+1}) = \Delta_{0, t_{j+1}}^{\gamma, \lambda(t)} v^{j+1} + \mathcal{O}(\tau^{2-\gamma}), \quad (2.1)$$

where $\Delta_{0, t_{j+1}}^{\gamma, \lambda(t)} u^{j+1} = \sum_{s=0}^j c_{j-s} [u(t_{s+1}) - u(t_s)]$ and $c_\ell = \frac{\tau^{-\gamma}}{\Gamma(2-\gamma)} [\lambda_{\ell+1/2}a_\ell + (\lambda_\ell - \lambda_{\ell+1})b_\ell]$ ($\ell \geq 0$). Moreover, the following inequalities hold:

$$a_0 > a_1 > \dots > a_\ell > \frac{1-\gamma}{(\ell+1)^\gamma}, \quad b_0 > b_1 > \dots > b_\ell > 0.$$

Based on the property of a_ℓ and b_ℓ , we can obtain the following result of the coefficients c_ℓ :

Lemma 2.2. For all $\ell = 0, 1, \dots$, $\gamma \in (0, 1)$ and $\lambda(t) \in \mathcal{C}^2[0, T]$, where $\lambda(t) > 0$, $\lambda'(t) \leq 0$ for all $t \in [0, T]$, the following inequalities hold:

$$c_0 > c_1 > \dots > c_\ell > \frac{\lambda(t_{\ell+1/2})}{\Gamma(1-\gamma)t_{\ell+1}^\gamma},$$

After we introduce the temporal discretization, it is the time to characterize the discretization in the space variable. First of all, we denote by

$$\mathcal{L}^{n+\alpha}(\mathbb{R}) = \left\{ v \mid v \in L_1(\mathbb{R}) \text{ and } \int_{-\infty}^{+\infty} (1+|k|)^{n+\beta} |\hat{v}(k)| dk < \infty \right\},$$

where $\hat{v}(k) = \int_{-\infty}^{+\infty} e^{\iota kx} v(x) dx$ is the Fourier transformation of $v(x)$, and by $\iota = \sqrt{-1}$ the imaginary unit. Then we introduce the following preliminary lemma, which provides numerical approximations for the spatial R-L fractional derivatives:

Lemma 2.3. Let $v(x) \in \mathcal{L}^{2+\alpha}(\mathbb{R})$ and define the following difference operators

$$\begin{aligned}\delta_{x,+}^\alpha v(x) &= \frac{1}{h^\alpha} \sum_{k=0}^{\lfloor \frac{x-a}{h} \rfloor} w_k^{(\alpha)} v(x - (k-1)h), \\ \delta_{x,-}^\alpha v(x) &= \frac{1}{h^\alpha} \sum_{k=0}^{\lfloor \frac{b-x}{h} \rfloor} w_k^{(\alpha)} v(x + (k-1)h),\end{aligned}$$

then, for a fixed h , we have

$${}_a D_x^\alpha v(x) = \delta_{x,+}^\alpha v(x) + \mathcal{O}(h^2) \quad \text{and} \quad {}_x D_x^\alpha v(x) = \delta_{x,-}^\alpha v(x) + \mathcal{O}(h^2),$$

where $\lfloor \cdot \rfloor$ is the floor function and

$$\begin{cases} w_0^{(\alpha)} = \kappa_1 g_0^{(\alpha)}, & w_1^{(\alpha)} = \kappa_1 g_1^{(\alpha)} + \kappa_0 g_0^{(0)}, \\ w_k^{(\alpha)} = \kappa_1 g_k^{(\alpha)} + \kappa_0 g_{k-1}^{(\alpha)} + \kappa_{-1} g_{k-2}^{(\alpha)}, & k \geq 2 \end{cases}$$

with

$$\kappa_1 = \frac{\alpha^2 + 3\alpha + 2}{12}, \quad \kappa_0 = \frac{4 - \alpha}{6}, \quad \kappa_{-1} = \frac{\alpha^2 - 3\alpha + 2}{12}, \quad \text{and} \quad g_k^{(\alpha)} = (-1)^k \binom{\alpha}{k}.$$

At this stage, the numerical approximations of both the temporal and spatial fractional deviates have been ready for deriving the target implicit difference scheme. Let $u(x, t) \in \mathcal{C}_{x,t}^{4,2}([a, b] \times [0, T])$ be a solution of the problem (1.1). Then we consider Eq. (1.1) at the set of grid points $(x, t) = (x_i, t_{j+1}) \in \bar{Q}_T$, $i = 1, 2, \dots, N-1$, $j = 0, 1, \dots, M-1$:

$${}_0^C D_t^{\gamma, \lambda(t)} u(x_i, t_{j+1}) = \xi(x_i, t_{j+1}) \left(p_a D_x^\alpha u(x, t) + (1-p)_x D_b^\alpha u(x, t) \right)_{(x_i, t_{j+1})} + f(x_i, t_{j+1}).$$

Let U be a grid function defined by

$$U_i^j := u(x_i, t_j) \quad \text{and} \quad f_i^j = f(x_i, t_j), \quad 0 \leq i \leq N, \quad 0 \leq j \leq M.$$

Using this notation and recalling Lemma 2.1 and Lemma 2.3, we can write the problem (1.1) at the grid points (x_i, t_{j+1}) as follows

$$\Delta_{0,t_{j+1}}^{\gamma, \lambda(t)} U_i^{j+1} = \xi_i^{j+1} \left(\delta_h^\alpha U_i^{j+1} \right) + f_i^{j+1} + R_i^{j+1}, \quad 1 \leq i \leq N-1, \quad 0 \leq j \leq M-1, \quad (2.2)$$

where $\{R_i^{j+1}\}$ are small and satisfy the relation $|R_i^{j+1}| = \mathcal{O}(\tau^{2-\gamma} + h^2)$ for $1 \leq i \leq N-1$, $0 \leq j \leq M-1$. We omit them and use the initial-boundary value conditions

$$\begin{cases} U_i^0 = \phi(x_i), & 1 \leq i \leq N-1, \\ U_0^j = \varphi(t_j), \quad U_N^j = \psi(t_j), & 0 \leq j \leq M. \end{cases}$$

For the sake of clarity, we introduce the notations

$$\xi_i^j = \xi(x_i, t_j), \quad \delta_h^\alpha u_i^{j+1} = \frac{1}{h^\alpha} \left[p \sum_{k=0}^{i+1} w_k^{(\alpha)} u_{i-k+1}^{j+1} + (1-p) \sum_{k=0}^{N-i+1} w_k^{(\alpha)} u_{i+k-1}^{j+1} \right],$$

and then we arrive at the implicit difference scheme with (local) truncation errors of $\mathcal{O}(\tau^{2-\gamma} + h^2)$:

$$\begin{cases} \Delta_{0,t_{j+1}}^{\gamma, \lambda(t)} u_i^{j+1} = \xi_i^{j+1} \left(\delta_h^\alpha u_i^{j+1} \right) + f_i^{j+1}, & i = 1, 2, \dots, N-1, \quad j = 0, 1, \dots, M-1, \\ u_i^0 = \phi(x_i), & i = 0, 1, \dots, N, \\ u_0^j = \varphi(t_j), \quad u_N^j = \psi(t_j), & j = 0, 1, \dots, M. \end{cases} \quad (2.3)$$

It is interesting to note that for $\lambda(t) \equiv 1$ and $\gamma \rightarrow 1$, Eq. (2.3) reduces to the classical backward Euler scheme for solving the SFDEs with variable coefficients [22, 48]. Similarly, if $\alpha = 2$, the above scheme (2.3) collapses to the implicit difference scheme introduced in [8] for solving the variable-coefficient GTFDEs.

2.2. Stability and convergence analysis

In this subsection, we are committed to analyzing both the stability and convergence for the implicit difference scheme (2.3). We define

$V_h = \{\mathbf{v} \mid \mathbf{v} = \{v_i\} \text{ is a grid function on } \varpi_h \text{ and } v_i = 0 \text{ if } i = 0, N\}$,

and, for all $\mathbf{u}, \mathbf{v} \in V_h$, the discrete inner product and corresponding discrete L^2 -norms

$$(\mathbf{u}, \mathbf{v}) = h \sum_{i=1}^{N-1} u_i v_i, \quad \text{and} \quad \|\mathbf{u}\| = \sqrt{(\mathbf{u}, \mathbf{u})}.$$

The starting point of our analysis is the following theoretical result.

Lemma 2.4. ([49, 50]) *Let $\alpha \in (1, 2)$ and $g_k^{(\alpha)}$ be defined in Lemma 2.3, then we obtain*

$$\begin{cases} w_0^{(\alpha)} = \kappa_1 > 0, & w_1^{(\alpha)} < 0, & w_k^{(\alpha)} > 0, & k \geq 3, \\ \sum_{k=0}^{\infty} w_k^{(\alpha)} = 0, & \sum_{k=0}^N w_k^{(\alpha)} < 0, & N > 1, \\ w_0^{(\alpha)} + w_2^{(\alpha)} \geq 0. \end{cases}$$

In fact, this lemma does not show whether $w_2^{(\alpha)}$ is positive or negative. After simple calculations, we obtain

$$\begin{aligned} w_2^{(\alpha)} &= \kappa_1 g_2^{(\alpha)} + \kappa_0 g_1^{(\alpha)} + \kappa_{-1} g_0^{(\alpha)} \\ &= \frac{\alpha^4}{24} + \frac{\alpha^3}{12} + \frac{5\alpha^2}{24} - \alpha + \frac{1}{6}, \end{aligned} \tag{2.4}$$

where $\alpha \in (1, 2]$ and it can be plotted as Fig. 1. As seen from Fig. 1, the following proposition can be

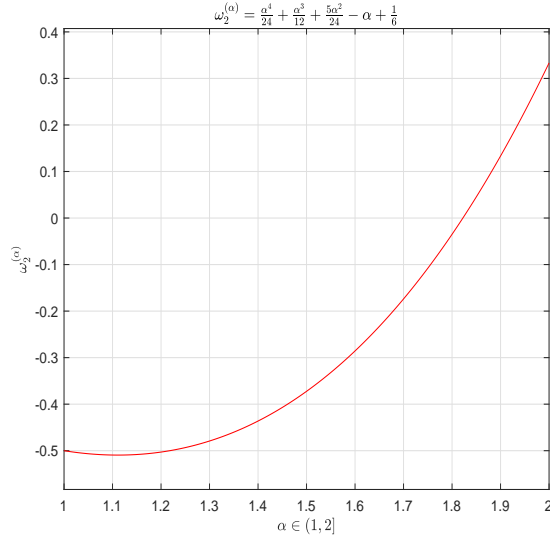


Fig. 1: The plot of $w_2^{(\alpha)}$ with $\alpha \in (1, 2]$.

derived, which is helpful to analyse the property of coefficient matrices of Eq. (3.3) in the next context.

Proposition 2.1. When $\alpha \in (1, \alpha_0)$, then $w_2^{(\alpha)} < 0$. Similarly, when $\alpha \in [\alpha_0, 2]$, then $w_2^{(\alpha)} \geq 0$ with $\alpha_0 \approx 1.8223$. Moreover, the sufficient condition for W_α and W_α^T to be diagonally dominant is $\alpha \in [\alpha_0, 2]$, where the matrix W_α is given as follows,

$$W_\alpha = \begin{pmatrix} w_1^{(\alpha)} & w_0^{(\alpha)} & 0 & \cdots & 0 & 0 \\ w_2^{(\alpha)} & w_1^{(\alpha)} & w_0^{(\alpha)} & 0 & \cdots & 0 \\ \vdots & w_2^{(\alpha)} & w_1^{(\alpha)} & \ddots & \ddots & \vdots \\ \vdots & \ddots & \ddots & \ddots & \ddots & 0 \\ w_{N-2}^{(\alpha)} & \ddots & \ddots & \ddots & w_1^{(\alpha)} & w_0^{(\alpha)} \\ w_{N-1}^{(\alpha)} & w_{N-2}^{(\alpha)} & \cdots & \cdots & w_2^{(\alpha)} & w_1^{(\alpha)} \end{pmatrix} \in \mathbb{R}^{(N-1) \times (N-1)}. \quad (2.5)$$

Proof. Since $\alpha \in [\alpha_0, 2]$, it holds $w_1^{(\alpha)} < 0$ and $w_k^{(\alpha)} \geq 0$ ($k \neq 1$). According to $\sum_{k=0}^{\infty} w_k^{(\alpha)} = 0$, it holds that both W_α and W_α^T are diagonally dominant [28]. \square

Based on Lemma 2.4, the first two properties of the discrete inner product related to two approximate operators $\delta_{x,+}^\alpha$ and $\delta_{x,-}^\alpha$ can be shown below.

Lemma 2.5. ([49, 50]) For $\alpha \in (1, 2)$ and $N \geq 5$, and any $\mathbf{v} \in V_h$, it holds that

$$(-\delta_{x,+}^\alpha \mathbf{v}, \mathbf{v}) = (-\delta_{x,-}^\alpha \mathbf{v}, \mathbf{v}) > c \ln 2 \|\mathbf{v}\|^2.$$

where c is positive constant independent of the spatial step size h .

Theorem 2.1. For $\alpha \in (1, 2)$, and any $\mathbf{v} \in V_h$, then it holds that

$$(\delta_h^\alpha \mathbf{v}, \mathbf{v}) < -c \ln 2 \|\mathbf{v}\|^2,$$

where c is the same as that in Lemma 2.5.

Proof. The concrete expression of $(\delta_h^\alpha \mathbf{v}, \mathbf{v})$ can be written as

$$(\delta_h^\alpha \mathbf{v}, \mathbf{v}) = p(\delta_{x,+}^\alpha \mathbf{v}, \mathbf{v}) + (1-p)(\delta_{x,-}^\alpha \mathbf{v}, \mathbf{v}) \leq -c \ln 2 \|\mathbf{v}\|_2,$$

then this completes the proof of Theorem 2.1. \square

To establish the stability of the difference scheme, we still need to introduce the following lemma,

Lemma 2.6. For any function $v(t)$ defined on the discrete grid $\varpi_\tau = \{t_j = j\tau : j = 0, 1, \dots, M\}$, the following inequality holds

$$\mathbf{v}^{j+1} (K^{j+1})^{-1} \Delta_{0,t_{j+1}}^{\gamma, \lambda(t)} \mathbf{v} \geq \frac{1}{2} \Delta_{0,t_{j+1}}^{\gamma, \lambda(t)} \|\mathbf{v}\|_{(K^{j+1})^{-1}}^2, \quad (2.6)$$

where $K^{j+1} = \text{diag}(\xi_1^{j+1}, \xi_2^{j+1}, \dots, \xi_{n-1}^{j+1}) > 0$ and $\|\mathbf{v}\|_{(K^{j+1})^{-1}}^2 = \mathbf{v}^T (K^{j+1})^{-1} \mathbf{v}$.

Proof. We rewrite the following inner product

$$\mathbf{v}^{j+1} (K^{j+1})^{-1} \Delta_{0,t_{j+1}}^{\gamma, \lambda(t)} \mathbf{v} = \tilde{\mathbf{v}}^{j+1} \Delta_{0,t_{j+1}}^{\gamma, \lambda(t)} \tilde{\mathbf{v}} \geq \frac{1}{2} \Delta_{0,t_{j+1}}^{\gamma, \lambda(t)} \|\tilde{\mathbf{v}}\|_2, \quad (2.7)$$

where $\tilde{\mathbf{v}} = (K^{j+1})^{-\frac{1}{2}} \mathbf{v}$ regarded as a (weighted) function $v(t)$ defined on the discrete grid ϖ_τ . Meanwhile, the inequality of (2.7) is correct due to [8, Lemma 4.4]. \square

Another ingredient introduced as the following lemma is also required to describe the diagonally weighted norm, which will be used in the next theorem.

Lemma 2.7. ([31]) Let $H \in \mathbb{R}^{n \times n}$ be a symmetric matrix with eigenvalues $\lambda_1 \geq \lambda_2 \geq \dots \geq \lambda_n$. Then for all $\mathbf{w} \in \mathbb{R}^{n \times 1}$,

$$\lambda_n \mathbf{w}^T \mathbf{w} \leq \mathbf{w}^T H \mathbf{w} \leq \lambda_1 \mathbf{w}^T \mathbf{w}. \quad (2.8)$$

Now we can conclude the stability and convergence of the implicit difference scheme (2.3). For simplicity of presentation, we denote $a_s^{j+1} = c_{j-s}$, then $\Delta_{0,t_{j+1}}^{\gamma,\lambda(t)} \mathbf{u} = \sum_{s=0}^j (\mathbf{u}^{s+1} - \mathbf{u}^s) a_s^{j+1}$.

Theorem 2.2. If we define Denote $\|\mathbf{f}^{j+1}\|^2 = h \sum_{i=1}^{N-1} f^2(x_i, t_{j+1})$, then the implicit difference scheme (2.3) is unconditionally stable and the following a priori estimate holds:

$$\|\mathbf{u}^{j+1}\|_{(K^{j+1})^{-1}}^2 \leq \frac{1}{\xi_{\min}} \left(\|\mathbf{u}^0\|^2 + \frac{\Gamma(1-\gamma)T^\gamma}{2c\xi_{\min} \ln 2\lambda(T)} \max_{0 \leq j \leq M-1} \|\mathbf{f}^{j+1}\|^2 \right) \quad (2.9)$$

where $\mathbf{u}^{j+1} = [u_1^{j+1}, u_2^{j+1}, \dots, u_{N-1}^{j+1}]^T$.

Proof. To make an inner product of Eq. (2.3) with \mathbf{u}^{j+1} , we have

$$(\Delta_{0,t_{j+1}}^{\gamma,\lambda(t)} \mathbf{u}, (K^{j+1})^{-1} \mathbf{u}^{j+1}) = (\delta_h^\alpha \mathbf{u}^{j+1}, \mathbf{u}^{j+1}) + (\mathbf{f}^{j+1}, (K^{j+1})^{-1} \mathbf{u}^{j+1}). \quad (2.10)$$

It follows from Theorem 2.1 and Lemma 2.6 that

$$(\delta_h^\alpha \mathbf{u}^{j+1}, \mathbf{u}^{j+1}) \leq -c \ln 2 \|\mathbf{u}^{j+1}\|^2 \quad (2.11)$$

and

$$(\Delta_{0,t_{j+1}}^{\gamma,\lambda(t)} \mathbf{u}, (K^{j+1})^{-1} \mathbf{u}^{j+1}) \geq \frac{1}{2} \Delta_{0,t_{j+1}}^{\gamma,\lambda(t)} \|\mathbf{u}\|_{(K^{j+1})^{-1}}^2. \quad (2.12)$$

Substituting (2.11)-(2.12) into (2.10) and using the Cauchy-Schwarz and Young's inequalities, we obtain

$$\begin{aligned} \frac{1}{2} \Delta_{0,t_{j+1}}^{\gamma,\lambda(t)} \|\mathbf{u}\|_{(K^{j+1})^{-1}}^2 &\leq -c \ln 2 \|\mathbf{u}^{j+1}\|^2 + (\mathbf{f}^{j+1}, (K^{j+1})^{-1} \mathbf{u}^{j+1}) \\ &\leq -c \ln 2 \|\mathbf{u}^{j+1}\|^2 + c\xi_{\min} \ln 2 \|\mathbf{u}^{j+1}\|_{(K^{j+1})^{-1}}^2 + \frac{1}{4c\xi_{\min} \ln 2} \|\mathbf{f}^{j+1}\|_{(K^{j+1})^{-1}}^2 \\ &\leq -c \ln 2 \|\mathbf{u}^{j+1}\|^2 + c \ln 2 \|\mathbf{u}^{j+1}\|^2 + \frac{1}{4c\xi_{\min} \ln 2} \|\mathbf{f}^{j+1}\|_{(K^{j+1})^{-1}}^2 \quad (\text{cf. Lemma 2.7}) \\ &= \frac{1}{4c\xi_{\min} \ln 2} \|\mathbf{f}^{j+1}\|_{(K^{j+1})^{-1}}^2. \end{aligned}$$

Next, we have the following inequality

$$a_j^{j+1} \|\mathbf{u}^{j+1}\|_{(K^{j+1})^{-1}}^2 \leq \sum_{s=1}^j (a_s^{j+1} - a_{s-1}^{j+1}) \|\mathbf{u}^s\|_{(K^{j+1})^{-1}}^2 + a_0^{j+1} \|\mathbf{u}^0\|_{(K^{j+1})^{-1}}^2 + \frac{1}{2c\xi_{\min} \ln 2} \|\mathbf{f}^{j+1}\|_{(K^{j+1})^{-1}}^2. \quad (2.13)$$

Employing the inequality $a_0^{j+1} = c_j > \frac{\lambda(T)}{\Gamma(1-\gamma)T^\gamma}$ (cf. [8, Theorem 5.1]), we obtain

$$\begin{aligned} a_j^{j+1} \|\mathbf{u}^{j+1}\|_{(K^{j+1})^{-1}}^2 &\leq \sum_{s=1}^j (a_s^{j+1} - a_{s-1}^{j+1}) \|\mathbf{u}^s\|_{(K^{j+1})^{-1}}^2 \\ &\quad + a_0^{j+1} \left(\|\mathbf{u}^0\|_{(K^{j+1})^{-1}}^2 + \frac{\Gamma(1-\gamma)T^\gamma}{2c\xi_{\min} \ln 2\lambda(T)} \|\mathbf{f}^{j+1}\|_{(K^{j+1})^{-1}}^2 \right). \end{aligned} \quad (2.14)$$

Suppose $h < 1$ and denote

$$\mathcal{P} \triangleq \frac{1}{\xi_{\min}} \left(\|\mathbf{u}^0\|^2 + \frac{\Gamma(1-\gamma)T^\gamma}{2c\xi_{\min} \ln 2\lambda(T)} \max_{0 \leq j \leq M-1} \|\mathbf{f}^{j+1}\|^2 \right).$$

Then, Eq. (2.14) can be rewritten as

$$a_j^{j+1} \|\mathbf{u}^{j+1}\|_{(K^{j+1})^{-1}}^2 \leq \sum_{s=1}^j (a_s^{j+1} - a_{s-1}^{j+1}) \|\mathbf{u}^s\|_{(K^{j+1})^{-1}}^2 + a_0^{j+1} \mathcal{P}. \quad (2.15)$$

At this stage, by mathematical induction we prove that

$$\|\mathbf{u}^s\|_{(K^{j+1})^{-1}}^2 \leq \mathcal{P}, \quad 0 \leq s \leq j+1 \quad (2.16)$$

is valid for the fixed j . The result is obviously true for $s = 0$ from (2.14). Assuming that (2.16) holds for all $0 \leq s \leq j$ ($0 \leq j \leq M-1$), then from (2.14) at $0 \leq s \leq j+1$, one has

$$\begin{aligned} a_j^{j+1} \|\mathbf{u}^{j+1}\|_{(K^{j+1})^{-1}}^2 &\leq \sum_{s=1}^j (a_s^{j+1} - a_{s-1}^{j+1}) \|\mathbf{u}^s\|_{(K^{j+1})^{-1}}^2 + a_0^{j+1} \mathcal{P} \\ &\leq \sum_{s=1}^j (a_s^{j+1} - a_{s-1}^{j+1}) \mathcal{P} + a_0^{j+1} \mathcal{P} \\ &= a_j^{j+1} \mathcal{P}, \end{aligned}$$

This completes the proof of Theorem 2.2. \square

The following theorem shows that our proposed implicit difference scheme achieves $(2-\gamma)$ -order and quadratic-order convergence in time and space variables, respectively, when the solution of Eq. (1.1) is sufficiently smooth. To our knowledge, it is the first theoretical result of the convergence of implicit difference schemes for solving the variable-coefficient GTSFDEs (1.1).

Theorem 2.3. Suppose that $u(x, t) \in \mathcal{C}_{x,t}^{4,2}([a, b] \times [0, T])$ is the solution of Eq. (1.1) and $\{u_i^j \mid x_i \in \varpi_h, 0 \leq j \leq M\}$ is the solution of the implicit difference scheme (2.3). Define

$$E_i^j = u(x_i, t_j) - u_i^j, \quad x_i \in \varpi_h, \quad 0 \leq j \leq M, \quad (2.17)$$

where $\varpi_h = \{x_i = ih, i = 0, 1, \dots, N; Nh = b - a\}$, then there exists a positive constant \tilde{c} such that

$$\|E^j\| \leq \tilde{c}(\tau^{2-\gamma} + h^2), \quad 0 \leq j \leq M.$$

Proof. It can be easily obtained that E^j satisfies the following error equation

$$\begin{cases} \Delta_{0,t_{j+1}}^{\gamma,\lambda(t)} E_i^{j+1} = \delta_h^\alpha E_i^{j+1} + R_i^{j+1}, & i = 1, 2, \dots, N-1, \quad j = 0, 1, \dots, M-1, \\ E_i^0 = 0, & i = 0, 1, \dots, N, \\ E_0^j = 0, \quad E_N^j = 0, & j = 0, 1, \dots, M, \end{cases} \quad (2.18)$$

where $\mathbf{R}^{j+1} = [R_1^{j+1}, R_2^{j+1}, \dots, R_{N-1}^{j+1}]^T$ and the truncation error term $\|\mathbf{R}^{j+1}\| = \mathcal{O}(\tau^{2-\gamma} + h^2)$. In virtue of Theorem 2.2 and Lemma 2.7, we define $\mathbf{E}^{j+1} = [E_1^{j+1}, E_2^{j+1}, \dots, E_{N-1}^{j+1}]^T$ and then arrive at

$$\|\mathbf{E}^{j+1}\|_{(K^{j+1})^{-1}}^2 \leq \frac{\Gamma(1-\gamma)T^\gamma}{2c\xi_{\min} \ln 2\lambda(T)} \|\mathbf{R}^{j+1}\|_{(K^{j+1})^{-1}}^2 \Rightarrow \|\mathbf{E}^{j+1}\| \leq \tilde{c}(\tau^{2-\gamma} + h^2), \quad 0 \leq j \leq M-1,$$

which proves the theorem. \square

Theorem 2.3 implies that our numerical scheme converges to the optimal order $\mathcal{O}(\tau^{2-\gamma} + h^2)$ in the L^2 -norm, when the solution of Eq. (1.1) is sufficiently smooth. Besides, if the solution of Eq. (1.1) is non-smooth, several useful alternatives utilizing the non-uniform temporal step or initial correction techniques [51–54] can be adapted to address this problem. However, that is not the emphasis of this current manuscript and we shall pursue that in the future work. In addition, the above analysis can be adopted to remedy defects in our previous work [50], which only focuses on the problem with time-varying diffusion coefficients.

3. Efficient implementation of the proposed implicit difference scheme

In order to develop efficient implementation of the proposed scheme, we rewrite the implicit difference scheme (2.3) into the following form with $i = 1, 2, \dots, N-1$ and $j = 0, 1, \dots, M-1$:

$$(c_0 u_i^{j+1} - c_j u_i^0) - \sum_{s=1}^j (c_{s-1} - c_s) u_i^{j+1-s} = \frac{\xi_i^{j+1}}{h^\alpha} \left[p \sum_{k=0}^{i+1} w_k^{(\alpha)} u_{i-k+1}^{j+1} + (1-p) \sum_{k=0}^{N-i+1} w_k^{(\alpha)} u_{i+k-1}^{j+1} \right] + f_i^{j+1}, \quad (3.1)$$

or equivalently

$$c_0 u_i^{j+1} - \frac{\xi_i^{j+1}}{h^\alpha} \left[p \sum_{k=0}^{i+1} w_k^{(\alpha)} u_{i-k+1}^{j+1} + (1-p) \sum_{k=0}^{N-i+1} w_k^{(\alpha)} u_{i+k-1}^{j+1} \right] = c_j u_i^0 + \sum_{s=1}^j (c_{s-1} - c_s) u_i^{j+1-s} + f_i^{j+1}. \quad (3.2)$$

At this stage, the above implicit difference scheme can be reformulated as the following sequence of linear systems,

$$\mathcal{M}^{(j+1)} \mathbf{u}^{j+1} = c_j \mathbf{u}^0 + \sum_{s=1}^j (c_{s-1} - c_s) \mathbf{u}^{j+1-s} + \mathbf{f}^{j+1}, \quad j = 0, 1, 2, \dots, M-1. \quad (3.3)$$

where $\mathcal{M}^{j+1} = c_0 I - \frac{K^{(j+1)}}{h^\alpha} [pW_\alpha + (1-p)W_\alpha^T]$, $\mathbf{u}^j = [u_1^j, u_2^j, \dots, u_{N-1}^j]^T$, $\mathbf{f}^j = [f_1^j, f_2^j, \dots, f_{N-1}^j]^T$, $K^{(j+1)} = \text{diag}(\xi_1^{j+1}, \xi_2^{j+1}, \dots, \xi_{N-1}^{j+1})$ and I is the identity matrix of order $(N-1)$. Meanwhile, it is obvious that W_α (2.5) is a Toeplitz matrix; refer to [22, 55]. Therefore, it can be stored with N entries and the matrix-vector product involving the matrix $\mathcal{M}^{(j)}$ can be evaluated via fast Fourier transforms (FFTs) in $\mathcal{O}(N \log N)$ operations [48, 55]. On the other hand, it is meaningful to remark that the sequence of linear systems (3.3) corresponding to the implicit scheme (2.3) is inherently sequential, thus it is difficult to parallelize over time. It implies that we need to solve the sequence of linear systems (3.3) one by one. Then the Krylov subspace method with suitable preconditioners [48, 56, 57] can be the efficient candidate for solving Toeplitz-like linear systems. In this case, it also remarked that the complexity of preconditioned Krylov subspace solvers is only in $\mathcal{O}(N \log N)$ arithmetic operations per iteration step.

In order to solve Eq. (3.3) well, we divide it into two specific classes:

- When the diffusion coefficient $\xi(x, t) \equiv \xi$, the coefficient matrix of Eq. (3.3) will be a time-independent Toeplitz matrix, i.e. $\mathcal{M}^{j+1} = \mathcal{M}$, then we can compute its matrix inverse via the Gohberg-Semencul formula (GSF) [58] using only its first and last columns, such a strategy does not need to call the preconditioned Krylov subspace solvers in each time level $0 \leq j \leq M-1$ and then the solution in each time level (i.e., $\mathcal{M}^{-1} \mathbf{u}^{j+1}$) can be calculated via about six FFTs, thus it can save the computational cost; refer to [32, 50, 59–61] for detail.
- When the diffusion coefficient is just a function related to both x and t , i.e., $\xi(x, t)$, the coefficient matrix of Eq. (3.3) becomes the sum of a scalar matrix and a diagonal-multiply-Toeplitz matrix, which is time-dependent. In this case, Eq. (3.3) has to be solved via the preconditioned Krylov subspace solver for each time level j .

Based on the above considerations, we still require to solve several nonsymmetric Toeplitz(-like) linear systems, whose matrix-vector products can be accessibly calculated via FFTs, thus we utilize the biconjugate gradient stabilized (BiCGSTAB) method which has a faster and smoother convergence [62]. For accelerating BiCGSTAB, we consider the following skew-circulant and band preconditioners:

$$P_{sk} = \begin{cases} c_0 I - \frac{\xi}{h^\alpha} [p \cdot sk(W_\alpha) + (1-p)sk(W_\alpha^T)], & \xi(x, t) \equiv \xi, \\ c_0 I - \frac{\xi^{(j+1)}}{h^\alpha} [p \cdot sk(W_\alpha) + (1-p)sk(W_\alpha^T)], & \xi^{(j+1)} = \frac{1}{N-1} \sum_{i=1}^{N-1} \xi(x_i, t_{j+1}), \end{cases} \quad (3.4)$$

where the vector $\delta = [w_1^{(\alpha)}, w_2^{(\alpha)}, \dots, w_{N-2}^{(\alpha)}, -w_0^{(\alpha)}]^T$ is the first column of the skew-circulant matrix $sk(W_\alpha)$ [59], and

$$P_b = \begin{cases} c_0 I - \frac{\xi}{h^\alpha} [pW_{\alpha,\ell} + (1-p)W_{\alpha,\ell}^T], & \xi(x, t) \equiv \xi, \\ c_0 I - \frac{K^{(j+1)}}{h^\alpha} [pW_{\alpha,\ell} + (1-p)W_{\alpha,\ell}^T], & \text{(general case)}, \end{cases} \quad (3.5)$$

with the band matrix

$$W_{\alpha,\ell} = \begin{bmatrix} w_1^{(\alpha)} & w_0^{(\alpha)} & & & \\ \vdots & w_1^{(\alpha)} & w_0^{(\alpha)} & & \\ w_\ell^{(\alpha)} & & \ddots & \ddots & \\ & \ddots & & \ddots & w_0^{(\alpha)} \\ & & w_\ell^{(\alpha)} & \dots & w_1^{(\alpha)} \end{bmatrix}, \quad \ell \in \mathbb{N}^+,$$

respectively. Meanwhile, the high efficiency of skew-circulant and banded preconditioners for (time-)space FDEs has been shown in [23, 46, 59].

For practical implementations, when P_{sk} or P_b is employed as the preconditioner, a fast preconditioned version BiCGSTAB method is obtained. During each BiCGSTAB iteration, two preconditioning steps are added in which one has to solve linear system $P_{sk}\mathbf{z} = \mathbf{y}$ or $P_b\mathbf{z} = \mathbf{y}$ for some given \mathbf{y} . Thus, some additional storage and computational cost are still required. However, we point out that P_{sk} (resp., P_b) can also be efficiently stored in $\mathcal{O}(N)$ (resp., $\mathcal{O}(\ell N)$) memory by only storing the $(N-1)$ -dimensional vector δ in (3.4) (resp., the band matrix $W_{\alpha,\ell}$ in (3.5)). Besides, as P_{sk} is the skew matrix¹, we observe that

$$P_{sk} = \Omega^* F^* \left(c_0 I - \frac{\xi^{(j+1)}}{h^\alpha} [p\Lambda_s + (1-p)\bar{\Lambda}_s] \right) F\Omega, \quad sk(W_\alpha) = \Omega^* F^* \Lambda_s F\Omega, \quad (3.6)$$

where $\Omega = \text{diag} \left(1, (-1)^{-\frac{1}{N-1}}, \dots, (-1)^{-\frac{N-2}{N-1}} \right)$, F is the discrete Fourier matrix and its conjugate transpose F^* . According to Eq. (3.6), the inverse-matrix-vector product $\mathbf{z} = P_{sk}^{-1}\mathbf{y}$ can be carried out in $\mathcal{O}(N \log N)$ operations via the (inverse) FFTs. Most importantly, the diagonal matrix Λ_s can be computed in advance and only one time during each time step. On the other hand, since $W_{\alpha,\ell}$ is a band matrix, then P_b should be a band matrix of bandwidth $2\ell + 1$ and $\mathbf{z} = P_b^{-1}\mathbf{y}$ can be computed by the banded LU decomposition [23, 46] in $\mathcal{O}(\ell N)$ arithmetic operations ($\ell \ll N$). In one word, we employ a fast preconditioned BiCGSTAB solution method with low memory requirement and computational cost per iteration, while the number of iterations and thus the total computational cost are greatly reduced. Compared to the skew-circulant preconditioner, the banded preconditioner needs more computational cost to update in each time level; refer to the next section for a discussion.

On the other hand, it is meaningful to note that when $\alpha \geq \alpha_0$, the coefficient matrix $\mathcal{M}^{(j+1)}$ are diagonally dominant with positive diagonal elements [28] due to Proposition 2.1 and $\xi(x, t) > 0$. Meanwhile, the banded preconditioner was shown to be considerably efficient for solving the linear systems with diagonally dominant coefficient matrix, which are from the numerical discretization of (time-)space FDEs; refer, e.g., to [23, 28, 46] for a discussion.

4. Numerical experiments

The numerical experiments presented in this section have a two-fold objective. They illustrate that the proposed implicit difference scheme (IDS) for the GTSFDE (1.1) can indeed converge with the order of

¹ If the diffusion coefficient $\xi(x, t) \equiv \xi$, then $\xi^{(j+1)}$ are time-varying constants, which is available for other similar cases.

$\mathcal{O}(\tau^{2-\gamma} + h^2)$. At the same time, they assess the computational efficiency of the fast solution techniques described in Section 3. For the Krylov subspace method and direct solver, we choose built-in functions for the preconditioned BiCGSTAB method, LU factorization of MATLAB in Example 1 (where $\xi(x, t) \equiv \xi$ and $\mathcal{M}^{(j+1)}$ will be independent of time levels) and MATLAB's backslash in Example 2 with variable coefficients (where the coefficient matrices $\mathcal{M}^{(j+1)}$ change in each time level), respectively. For the BiCGSTAB method with two different preconditioners, the stopping criterion of those methods is $\|\mathbf{r}^{(k)}\|_2 / \|\mathbf{r}^{(0)}\|_2 \leq 10^{-12}$, where $\mathbf{r}^{(k)}$ is the residual vector of the linear system after k iterations, and the initial guess is chosen as the zero vector. All experiments were performed on a Windows 10 (64 bit) PC-Intel(R) Core(TM) i5-8250U CPU @1.60 GHz–1.80GHz, 8 GB of RAM using MATLAB 2017b with machine epsilon 10^{-16} in double precision floating point arithmetic. By the way, all timings (measured in seconds) are averages over 20 runs of our algorithms. Before we report the numerical results of the IDS for the problem (1.1), some notations should be introduced as follows:

$$\text{Error}_\infty = \max_{0 \leq j \leq M} \|\mathbf{E}^j\|_\infty \quad \text{and} \quad \text{Error}_2 = \max_{0 \leq j \leq M} \|\mathbf{E}^j\|_2,$$

then

$$\text{Rate}_\infty = \begin{cases} \log_{\tau_1/\tau_2} \left(\frac{\text{Error}_{\infty, \tau_1}}{\text{Error}_{\infty, \tau_2}} \right), & (\text{temporal convergence order}), \\ \log_{h_1/h_2} \left(\frac{\text{Error}_{\infty, h_1}}{\text{Error}_{\infty, h_2}} \right), & (\text{spatial convergence order}), \end{cases}$$

and

$$\text{Rate}_2 = \begin{cases} \log_{\tau_1/\tau_2} \left(\frac{\text{Error}_{2, \tau_1}}{\text{Error}_{2, \tau_2}} \right), & (\text{temporal convergence order}), \\ \log_{h_1/h_2} \left(\frac{\text{Error}_{2, h_1}}{\text{Error}_{2, h_2}} \right), & (\text{spatial convergence order}). \end{cases}$$

Example 1. In this example, we study the GTSFDE problem (1.1) of order α with $\lambda(t) = e^{-bt}$, $b \geq 0$. The spatial domain is $[x_L, x_R] = [0, 1]$ and the time interval is $[0, T] = [0, 1]$. The diffusion coefficient function is defined as $\xi(x, t) \equiv \kappa$, $0 < p < 1$. The source term is

$$f(x, t) = \frac{10t^{3-\gamma}e^{-bt}}{\Gamma(4-\gamma)}x^2(1-x)^2 - 5\kappa g(t) \left\{ \frac{\Gamma(3)}{\Gamma(3-\alpha)} [px^{2-\alpha} + (1-p)(1-x)^{2-\alpha}] \right. \\ \left. - \frac{2\Gamma(4)}{\Gamma(4-\alpha)} [px^{3-\alpha} + (1-p)(1-x)^{3-\alpha}] + \frac{\Gamma(5)}{\Gamma(5-\alpha)} [px^{4-\alpha} + (1-p)(1-x)^{4-\alpha}] \right\},$$

and the initial-boundary value conditions are

$$u(x, 0) = 5g(0)x^2(1-x)^2, \quad \text{and} \quad u(0, t) = u(1, t) = 0.$$

The exact solution of this problem is $u(x, t) = 5g(t)x^2(1-x)^2$, where

$$g(t) = 1 + \frac{2 - (2 + 2bt + b^2t^2)e^{-bt}}{b^3}$$

for any $\alpha \in (1, 2)$ and $b \in \mathbb{R}^+$. Numerical results of the proposed scheme for the GTSFDE problem (1.1) with above conditions will be reported in the following Tables 1–4.

As seen from Tables 1–2, we report the maximum-norm errors, L_2 -norm errors of the IDS for solving the problem (1.1) with the constant diffusion coefficient in spatial and temporal directions, respectively. More precisely, Table 1 with different (γ, α, b) 's shows that if $h = 2^{-13}$, then as the number of time steps of our IDS is increased, a reduction in the maximum- or L_2 -norm error occurs as expected, and the temporal convergence order of IDS is $\mathcal{O}(\tau^{2-\gamma})$. At the same time, Table 2 with different (γ, α, b) 's displays that if $\tau = 2^{-9}$, then as the size of time steps of our IDS is decreased, a reduction in the maximum- or L_2 -norm error occurs as expected, and thus the convergence order of space is $\mathcal{O}(h^2)$. In conclusion, the numerical convergence orders are consistent with the theoretical estimate $\mathcal{O}(\tau^{2-\gamma} + h^2)$ described in Section 2.2.

Table 1: L_2 -norm and maximum norm errors versus grid size reduction when $h = 2^{-13}$, $\kappa = 5$, and $p = 0.3$ in Example 1.

(γ, α)	τ	$b = 1.0$				$b = 2.0$			
		Error $_{\infty}$	Rate $_{\infty}$	Error $_2$	Rate $_2$	Error $_{\infty}$	Rate $_{\infty}$	Error $_2$	Rate $_2$
(0.2,1.1)	1/8	6.1077e-5	–	4.1961e-5	–	3.0013e-5	–	2.0635e-5	–
	1/16	1.7691e-5	1.7876	1.2156e-5	1.7874	8.6743e-6	1.7908	5.9634e-6	1.7909
	1/32	5.1544e-6	1.7791	3.5438e-6	1.7783	2.5182e-6	1.7844	1.7326e-6	1.7832
	1/64	1.5100e-6	1.7713	1.0396e-6	1.7693	7.3995e-7	1.7669	5.1027e-7	1.7636
(0.5,1.5)	1/8	7.0570e-5	–	5.0000e-5	–	3.3908e-5	–	2.4008e-5	–
	1/16	2.5268e-5	1.4817	1.7901e-5	1.4819	1.2302e-5	1.4627	8.7114e-6	1.4625
	1/32	9.0351e-6	1.4837	6.3994e-6	1.4840	4.4079e-6	1.4807	3.1196e-6	1.4815
	1/64	3.2289e-6	1.4845	2.2852e-6	1.4856	1.5842e-6	1.4763	1.1197e-6	1.4782
(0.9,1.9)	1/8	1.3800e-4	–	9.6565e-5	–	6.8078e-5	–	4.7627e-5	–
	1/16	6.4618e-5	1.0947	4.5218e-5	1.0946	3.1853e-5	1.0958	2.2289e-5	1.0954
	1/32	3.0161e-5	1.0993	2.1106e-5	1.0992	1.4958e-5	1.0905	1.0466e-5	1.0906
	1/64	1.4075e-5	1.0995	9.8494e-6	1.0995	6.9963e-6	1.0963	4.8953e-6	1.0962

Table 2: L_2 -norm and maximum norm errors versus grid size reduction when $\tau = 2^{-9}$, $\kappa = 5$, and $p = 0.3$ in Example 1.

(γ, α)	h	$b = 1.0$				$b = 2.0$			
		Error $_{\infty}$	Rate $_{\infty}$	Error $_2$	Rate $_2$	Error $_{\infty}$	Rate $_{\infty}$	Error $_2$	Rate $_2$
(0.2,1.1)	1/4	1.6240e-1	–	8.8966e-2	–	1.5521e-1	–	8.5458e-2	–
	1/8	3.7465e-2	2.1159	2.3555e-2	1.9172	3.5981e-2	2.1089	2.2596e-2	1.9191
	1/16	8.4110e-3	2.1552	5.7795e-3	2.0270	8.1109e-3	2.1493	5.5529e-3	2.0248
	1/32	2.1057e-3	1.9980	1.3864e-3	2.0596	2.1056e-3	1.9456	1.3331e-3	2.0585
(0.5,1.5)	1/4	1.1062e-1	–	7.0677e-2	–	1.0430e-1	–	6.6713e-2	–
	1/8	2.4105e-2	2.1982	1.6211e-2	2.1243	2.2716e-2	2.1990	1.5278e-2	2.1265
	1/16	5.5961e-3	2.1068	3.7718e-3	2.1036	5.2688e-3	2.1082	3.5521e-3	2.1047
	1/32	1.3310e-3	2.0719	8.8855e-4	2.0857	1.2531e-3	2.0720	8.3631e-4	2.0866
(0.9,1.9)	1/4	9.5275e-2	–	6.7822e-2	–	8.9157e-2	–	6.3468e-2	–
	1/8	2.2929e-2	2.0549	1.6364e-2	2.0512	2.1452e-2	2.0552	1.5309e-2	2.0516
	1/16	5.5839e-3	2.0378	3.9677e-3	2.0442	5.2229e-3	2.0382	3.7112e-3	2.0444
	1/32	1.3659e-3	2.0314	9.6555e-4	2.0389	1.2768e-3	2.0323	9.0255e-4	2.0398

In Tables 3–4, we assess the performance of the direct, iterative, and preconditioned iterative methods for Eq. (3.3) in terms of CPU time and the average number of iterations. Here the symbols “Direct”, “Noprec”, “Banded($\ell = 8$)” and “Skew-cir” represent that we solve two fundamental equations of GSF [58] via the LU decomposition/BiCGSTAB with no preconditioner, banded preconditioner and skew-circulant preconditioner, respectively. Moreover, the symbol “†” means that the BiCGSTAB cannot converge within the maximum number (namely 2000) of iterations. This notation is used throughout this section. As can be seen from Tables 3–4, both banded and skew-circulant preconditioners are efficient to accelerate the BiCGSTAB methods in terms of the elapsed CPU time and the number of iterations, however the acceleration merit of these preconditioners (i.e., P_{sk} and P_b) is not very evident for small-scale problems. Moreover, it can be observed that the performance of P_{sk} is more robust than that of P_b in terms of the average number of iterations, i.e., compared to BiCGSTAB with P_b , the average of number of BiCGSTAB with P_{sk} is weakly sensitive to spatial grid size. In addition, it can be observed that when $\alpha = 1.9$, it seems that the performance of BiCGSTAB with P_b becomes better, because the banded preconditioner has been verified to be efficient for solving two fundamental equations of GSF [58, 59], whose the coefficient matrix is diagonally dominant – cf. Proposition 2.1 and Section 3 for a discussion. In summary, the skew-circulant preconditioner is still recommended for accelerating the convergence of BiCGSTAB in this example.

Table 3: Numerical comparisons of the direct, iterative, and preconditioned iterative methods for solving Example 1 with $b = 1.0$, $\tau = 2^{-12}$, $\kappa = 5$, and $p = 0.3$.

(γ, α)	N	Direct		Noprec		Banded($\ell = 8$)		Skew-cir	
		CPU(s)		Iter	CPU(s)	Iter	CPU(s)	Iter	CPU(s)
(0.2, 1.1)	64	15.487		303.0	15.498	10.0	15.642	12.0	15.519
	128	18.897		457.0	18.234	14.0	18.118	12.0	18.127
	256	24.388		890.0	22.187	17.0	22.059	14.0	22.067
	512	37.423		1826.0	30.029	24.0	29.702	14.0	29.538
	1024	75.449		†	†	39.0	44.325	14.0	44.284
(0.5, 1.5)	64	14.496		88.0	14.618	10.0	14.376	13.0	14.384
	128	16.758		167.0	16.729	15.0	16.701	14.0	16.661
	256	21.973		319.0	21.167	23.0	21.149	15.0	21.026
	512	30.843		678.0	29.821	36.0	29.635	16.0	29.446
	1024	51.375		1524.0	44.632	60.0	43.967	15.0	43.818
(0.9, 1.9)	64	14.535		95.0	14.448	6.0	14.259	10.0	14.403
	128	16.641		158.0	16.639	8.0	16.615	10.0	16.588
	256	21.225		319.0	21.506	10.0	21.213	12.0	21.207
	512	30.692		559.0	29.374	15.0	29.239	12.0	29.201
	1024	49.578		1217.0	44.081	26.0	43.967	14.0	43.879

Example 2. In this example, we solve the initial-boundary value problem of GTSFDE (1.1) with variable coefficients and $\lambda(t) = e^{-bt}$, $b \geq 0$, the spatial domain $[x_L, x_R] = [0, 2]$ and the time interval is $[0, T] = [0, 1]$. The diffusion coefficient function is given as $\xi(x, t) = 1 + x^2 + \sin t$. The source term is

$$f(x, t) = \frac{2t^{3-\gamma}e^{-bt}}{\Gamma(4-\gamma)}x^2(2-x)^2 - g(t)\xi(x, t)\left\{\frac{4\Gamma(3)}{\Gamma(3-\alpha)}\left[px^{2-\alpha} + (1-p)(2-x)^{2-\alpha}\right] - \frac{4\Gamma(4)}{\Gamma(4-\alpha)}\left[px^{3-\alpha} + (1-p)(2-x)^{3-\alpha}\right] + \frac{\Gamma(5)}{\Gamma(5-\alpha)}\left[px^{4-\alpha} + (1-p)(2-x)^{4-\alpha}\right]\right\},$$

and the initial-boundary value conditions are

$$u(x, 0) = g(0)x^2(2-x)^2, \quad \text{and} \quad u(0, t) = u(2, t) = 0.$$

The exact solution of this problem is $u(x, t) = g(t)x^2(2-x)^2$, where $g(t)$ is the same as Example 1. Numerical results will be displayed in the following Tables 5–8.

As seen from Tables 5–6, we show the maximum-norm errors, L_2 -norm errors of the IDS for solving the problem (1.1) with variable diffusion coefficients in spatial and temporal variables, respectively. More precisely, Table 5 with different (γ, α, b) 's gives that if $h = 2^{-12}$, then as the number of time steps of our IDS is increased, a reduction in the maximum- or L_2 -norm error occurs as expected, and the temporal convergence order of IDS is $\mathcal{O}(\tau^{2-\gamma})$. At the same time, Table 2 with different (γ, α, b) 's displays that if $\tau = 2^{-10}$, then as the size of time steps of our IDS is decreased, a reduction in the maximum- or L_2 -norm error occurs as expected, and thus the convergence order of space is $\mathcal{O}(h^2)$. In conclusion, the numerical convergence orders are consistent with the theoretical estimate $\mathcal{O}(\tau^{2-\gamma} + h^2)$ described in Section 2.2.

In Tables 7–8, the performance of the direct, iterative, and preconditioned iterative methods for Eq. (3.3) are shown along with the elapsed CPU time and the average number of iterations. Here the symbols “Direct”, “Noprec”, “Banded($\ell = 8$)” and “Skew-cir” represent that the sequence of linear systems (3.3) is consecutively solved via the MATLAB’s backslash/BiCGSTAB with no preconditioner, banded preconditioner and skew-circulant preconditioner, respectively. As can be seen from Tables 7–8, both banded and skew-circulant preconditioners are fairly efficient to accelerate the BiCGSTAB methods for Eq. (3.3) in terms of the elapsed CPU time and the number of iterations, especially when the number of grid nodes increases. Moreover, it remarked that the performance of P_{sk} is more robust than that of P_b in terms of the

Table 4: Numerical comparisons of the direct, iterative, and preconditioned iterative methods for solving Example 1 with $b = 2.0$, $\tau = 2^{-12}$, $\kappa = 5$, and $p = 0.7$.

(γ, α)	N	Direct		Noprec		Banded($\ell = 8$)		Skew-cir	
		CPU(s)		Iter	CPU(s)	Iter	CPU(s)	Iter	CPU(s)
(0.2,1.1)	64	15.054		307.0	14.471	10.0	14.391	12.0	14.374
	128	17.134		460.0	17.121	14.0	17.010	12.0	17.004
	256	22.549		909.0	21.052	17.0	21.027	14.0	20.911
	512	38.091		1813.0	30.018	24.0	29.233	14.0	29.092
	1024	76.272		†	†	39.0	43.967	14.0	43.767
(0.5,1.5)	64	15.203		88.0	15.079	10.0	14.939	13.0	14.876
	128	18.420		166.0	17.654	15.0	17.492	14.0	17.463
	256	22.076		307.0	21.978	23.0	21.826	15.0	21.750
	512	31.651		638.0	29.335	36.0	29.195	16.0	29.088
	1024	50.219		1524.0	44.667	60.0	44.372	15.0	44.123
(0.9,1.9)	64	14.898		96.0	14.901	6.0	14.788	10.0	14.756
	128	17.383		161.0	17.238	8.0	17.190	12.0	17.178
	256	22.081		300.0	21.984	10.0	21.893	12.0	21.851
	512	31.914		564.0	29.726	15.0	29.428	12.0	29.352
	1024	50.402		1170.0	46.955	26.0	44.716	13.0	44.598

Table 5: L_2 -norm and maximum norm errors versus grid size reduction when $h = 2^{-12}$ and $p = 0.7$ in Example 2.

(γ, α)	τ	$b = 1.0$				$b = 2.0$			
		Error $_{\infty}$	Rate $_{\infty}$	Error $_2$	Rate $_2$	Error $_{\infty}$	Rate $_{\infty}$	Error $_2$	Rate $_2$
(0.2,1.1)	1/8	5.9654e-4	–	5.5779e-4	–	3.1311e-4	–	2.9126e-4	–
	1/16	1.7385e-4	1.7788	1.6250e-4	1.7793	9.0388e-5	1.7925	8.4009e-5	1.7937
	1/32	5.0703e-5	1.7777	4.7379e-5	1.7781	2.6194e-5	1.7869	2.4335e-5	1.7875
	1/64	1.4813e-5	1.7752	1.3843e-5	1.7751	7.6240e-6	1.7806	7.0838e-6	1.7804
(0.5,1.5)	1/8	1.0328e-3	–	1.0162e-3	–	5.1328e-4	–	5.0407e-4	–
	1/16	3.7458e-4	1.4632	3.6869e-4	1.4627	1.8639e-4	1.4614	1.8284e-4	1.4630
	1/32	1.3450e-4	1.4777	1.3235e-4	1.4781	6.7060e-5	1.4748	6.5809e-5	1.4742
	1/64	4.8098e-5	1.4836	4.7330e-5	1.4835	2.4016e-5	1.4815	2.3557e-5	1.4821
(0.9,1.9)	1/8	2.9303e-3	–	2.8851e-3	–	1.3940e-3	–	1.3710e-3	–
	1/16	1.3909e-3	1.0750	1.3700e-3	1.0744	6.6816e-4	1.0610	6.5664e-4	1.0621
	1/32	6.5575e-4	1.0848	6.4585e-4	1.0849	3.1678e-4	1.0767	3.1149e-4	1.0759
	1/64	3.0744e-4	1.0928	3.0279e-4	1.0929	1.4894e-4	1.0887	1.4650e-4	1.0883

average number of iterations, i.e., compared to BiCGSTAB with P_b , the average of number of BiCGSTAB with P_{sk} is weakly sensitive to spatial grid size. In addition, it can be observed that when $\alpha = 1.9$, it seems that the performance of BiCGSTAB with P_b becomes better, because the banded preconditioner has been verified to be very efficient for solving the Eq. (3.3), whose coefficient matrices are diagonally dominant – cf. Proposition 2.1 and Section 3 for a discussion. In conclusion, the skew-circulant preconditioner is still recommended for enhancing the convergence of BiCGSTAB applied to solve Eq. (3.3), when $1 < \alpha < \alpha_0$. Whereas the banded preconditioner will be recommended if $\alpha \geq \alpha_0$, because the coefficient matrices become diagonally dominant – cf. Section 3.

In addition, according to numerical results of Examples 1-2, it is interesting to find that although we employ the fast preconditioned BiCGSTAB method to solve Eq. (3.3) corresponding to the IDS (2.3), the total CPU time of our proposed methods is still high. In fact, the total CPU time comes from two main parts: 1) solve the sequence of linear systems (3.3); 2) evaluate the right-hand side vector of (3.3) via summing the solutions of previous time levels repeatedly. Our preconditioned BiCGSTAB method can only alleviate

Table 6: L_2 -norm and maximum norm errors versus grid size reduction when $\tau = 2^{-10}$ and $p = 0.7$ in Example 2.

(γ, α)	h	$b = 1.0$				$b = 2.0$			
		Error $_{\infty}$	Rate $_{\infty}$	Error $_2$	Rate $_2$	Error $_{\infty}$	Rate $_{\infty}$	Error $_2$	Rate $_2$
(0.2, 1.1)	2/8	1.0332e-1	–	9.5781e-2	–	1.0756e-1	–	9.6687e-2	–
	2/16	2.4194e-2	2.0944	2.3302e-2	2.0393	2.3916e-2	2.1691	2.3510e-2	2.0400
	2/32	7.3546e-3	1.7180	5.5686e-3	2.0650	6.6797e-3	1.8401	5.6175e-3	2.0653
	2/64	2.0330e-3	1.8550	1.3355e-3	2.0599	1.8355e-3	1.8636	1.3477e-3	2.0594
(0.5, 1.5)	2/8	7.0414e-2	–	6.7030e-2	–	6.9027e-2	–	6.5647e-2	–
	2/16	1.6525e-2	2.0912	1.5689e-2	2.0951	1.6114e-2	2.0988	1.5317e-2	2.0996
	2/32	3.9248e-3	2.0740	3.7129e-3	2.0791	3.8292e-3	2.0732	3.6158e-3	2.0827
	2/64	1.0322e-3	1.9269	8.8843e-4	2.0632	9.5842e-4	1.9983	8.6283e-4	2.0672
(0.9, 1.9)	2/8	6.9963e-2	–	7.0620e-2	–	6.6930e-2	–	6.7553e-2	–
	2/16	1.7061e-2	2.0359	1.7145e-2	2.0423	1.6307e-2	2.0372	1.6387e-2	2.0435
	2/32	4.1828e-3	2.0282	4.1803e-3	2.0361	3.9886e-3	2.0315	3.9871e-3	2.0391
	2/64	1.0354e-3	2.0143	1.0281e-3	2.0236	9.7927e-4	2.0261	9.7271e-4	2.0353

the cost of 1), it implies that we further consider how to degrade the CPU time for handling the nonlocal property of the discrete temporal fractional derivative. However, its derivation and theoretical analysis are always difficult to the general case of $\lambda(t)$. In particular, if we set $\lambda(t) = e^{-bt}$ like the setting of Examples 1-2, we can further alleviate the computational and memory cost of the proposed IDS, the derivation of such a “economic” scheme (A.5) is a bit lengthy and is moved to Appendix A.

5. Conclusions

In this paper, the stability and convergence of an IDS for solving the GTSFDEs with variable coefficients are studied via the diagonally weighted energy norm analysis. The proposed IDS can be proved to reach the convergence of the second order in space and the $(2 - \gamma)$ -th approximation order in time for the GTSFDEs with variable coefficients. Moreover, numerical experiments completely supporting the obtained theoretical results are carried out. The method can be easily extended to solve the variable coefficient GTSFDEs with other boundary conditions. Although the focus is on the case of the one-dimensional spatial domain in this work, we note that the results can be extended for two- and three-dimensional cases; refer, e.g., to [49].

In addition, we have also shown an efficient implementation of the proposed IDS based on preconditioned iterative solvers, achieving about $\mathcal{O}(N \log N)$ computational complexity and $\mathcal{O}(N)$ storage cost. Numerical experiments are reported to show the efficiency of the proposed preconditioning methods. For special choice of $\lambda(t) = e^{-bt}$, the fast sum-of-exponential approximations of the kernel used in (1.2) can be used to derive a “economic” version of IDS (A.5), then numerical experiments are shown that the rate of the truncation error of this new IDS is about $\mathcal{O}(\tau^{2-\gamma} + h^2)$, however its rigorous stability and convergence analyses remain an open question. Meanwhile, numerical results show the fast IDS (A.5) requires less CPU time and memory cost than the proposed IDS (2.3).

Appendix A. Fast SOE approximation of the generalized Caputo fractional derivative

Due to the nonlocality of the generalized Caputo fractional derivative (1.2), the proposed scheme (3.3) requires the storage of the solution at all previous time steps which leads to huge computational cost. This phenomenon also can be observed from numerical experiments reported in Section 4. To reduce the computational cost, we follow the work about fast $L1$ formula [47] for develop the fast SOE approximation

Table 7: Numerical comparisons of the direct, iterative, and preconditioned iterative methods for solving Example 2 with $\tau = 2^{-12}$, $b = 1.0$, and $p = 0.7$.

(γ, α)	N	Direct	Noprec		Banded($\ell = 8$)		Skew-cir	
		CPU(s)	Iter	CPU(s)	Iter	CPU(s)	Iter	CPU(s)
(0.2,1.1)	64	20.128	98.1	33.527	5.0	19.681	13.6	20.942
	128	25.895	225.0	84.890	6.0	23.462	13.8	26.027
	256	55.777	994.5	893.026	7.3	32.152	14.3	31.613
	512	249.966	†	†	9.9	54.337	15.0	56.042
	1024	1859.940	†	†	16.2	102.047	15.6	75.748
(0.5,1.5)	64	18.203	33.9	21.434	4.0	19.748	12.1	20.401
	128	25.666	65.0	38.702	5.5	23.111	14.1	26.180
	256	52.250	127.6	68.884	8.0	32.794	14.8	31.585
	512	249.797	261.8	311.449	11.7	57.665	15.6	57.493
	1024	1836.925	999.9	3358.602	18.7	109.722	16.3	77.504
(0.9,1.9)	64	17.178	19.3	18.399	2.0	17.237	9.4	18.824
	128	24.118	39.0	29.815	3.0	21.174	12.0	24.843
	256	52.021	71.8	49.841	4.0	26.891	13.4	30.941
	512	260.412	147.4	183.047	5.0	42.013	14.8	55.654
	1024	1835.804	301.3	421.588	7.0	70.558	15.7	76.047

Table 8: Numerical comparisons of the direct, iterative, and preconditioned iterative methods for solving Example 2 with $\tau = 2^{-12}$, $b = 2.0$ and $p = 0.3$.

(γ, α)	N	Direct	Noprec		Banded($\ell = 8$)		Skew-cir	
		CPU	Iter	CPU	Iter	CPU	Iter	CPU
(0.2,1.1)	64	19.850	84.9	30.368	5.0	19.153	14.9	20.935
	128	26.045	204.3	80.795	5.5	23.267	15.9	26.447
	256	54.872	981.7	1017.883	7.3	30.687	15.9	32.356
	512	250.823	†	†	11.0	57.626	15.8	57.388
	1024	1822.899	†	†	17.8	107.799	16.6	77.719
(0.5,1.5)	64	19.678	30.9	20.937	4.2	18.334	12.5	19.637
	128	26.470	60.0	36.100	5.4	23.145	14.2	26.188
	256	54.736	123.1	67.480	7.8	33.156	14.8	31.489
	512	260.543	246.8	293.753	11.3	57.874	14.9	55.981
	1024	1824.693	502.1	658.004	18.9	110.868	15.8	76.082
(0.9,1.9)	64	18.577	19.1	19.245	2.0	18.172	9.2	19.026
	128	24.914	39.4	30.340	3.0	22.314	11.9	24.145
	256	52.028	70.3	47.876	3.0	27.789	13.6	30.749
	512	250.682	144.2	175.927	5.0	42.018	14.9	55.671
	1024	1823.420	298.9	410.570	7.0	70.534	15.9	75.984

of the generalized Caputo fractional derivative with $\lambda(t) = e^{-bt}$, which is using in Section 4. More precisely,

$$\begin{aligned}
{}_0^C D_t^{\gamma, \lambda(t)} u(t) |_{t=t_j} &= \frac{1}{\Gamma(1-\gamma)} \int_0^{t_j} \frac{e^{-b(t_j-s)} u'(s) ds}{(t_j-s)^\gamma} \\
&= \frac{1}{\Gamma(1-\gamma)} \int_{t_{j-1}}^{t_j} \frac{e^{-b(t_j-s)} u'(s) ds}{(t_j-s)^\gamma} + \frac{1}{\Gamma(1-\gamma)} \int_0^{t_{j-1}} \frac{e^{-b(t_j-s)} u'(s) ds}{(t_j-s)^\gamma} \\
&= C_l(t_j) + C_h(t_j),
\end{aligned}$$

where the last equality defines the local part and the history part, respectively. For the local part, we employ the generalized $L1$ approximation recalled in Section 2.1, which approximates $u(s)$ on $[t_{j-1}, t_j]$ via a linear polynomial (with $u(t_{j-1})$ and $u(t_j)$ as the interpolation nodes) or $u'(s)$ via a constant $\frac{u(t_j)-u(t_{j-1})}{\tau}$. We have

$$\begin{aligned} C_l(t_j) &\approx \frac{u(t_j) - u(t_{j-1})}{\tau\Gamma(1-\gamma)} \int_{t_{j-1}}^{t_j} \frac{e^{-b(t_j-s)} ds}{(t_j-s)^\gamma} \\ &= \frac{u(t_j) - u(t_{j-1})}{\tau\Gamma(2-\gamma)} \left(e^{-b\tau} \tau^{1-\gamma} + b \int_0^\tau e^{-b\theta} \theta^{1-\gamma} d\theta \right), \end{aligned} \quad (\text{A.1})$$

where the second integral can be evaluated via the MATLAB built-in function ‘`integral.m`’. For the history part, we first recall the following lemma [47] to approximate the history part $C_h(t_j)$.

Lemma Appendix A.1. *Let ϵ denote tolerance error, δ cut-off time restriction and T final time. Then there are a natural number N_{exp} and positive numbers s_k and w_k , $k = 1, 2, \dots, N_{exp}$ such that*

$$\left| \frac{1}{t^\gamma} - \sum_{k=1}^{N_{exp}} \omega_k e^{-s_k t} \right| < \epsilon, \quad \text{for any } t \in [\delta, T],$$

where $N_{exp} = \mathcal{O}((\log \epsilon^{-1})(\log \log \epsilon^{-1} + \log(T\delta^{-1})) + (\log \delta^{-1})(\log \log \epsilon^{-1} + \log \delta^{-1}))$.

Therefore, when we set $\delta = \tau$ and apply Lemma Appendix A.1, then we obtain

$$\begin{aligned} C_h(t_j) &\approx \frac{1}{\Gamma(1-\gamma)} \int_0^{t_{j-1}} e^{-b(t_j-s)} \sum_{k=1}^{N_{exp}} \omega_k e^{-s_k(t_j-s)} u'(s) ds \\ &\triangleq \frac{1}{\Gamma(1-\gamma)} \sum_{k=1}^{N_{exp}} \int_0^{t_{j-1}} \omega_k e^{-\tilde{s}_k(t_j-s)} u'(s) ds \quad \left(\triangleq \frac{1}{\Gamma(1-\gamma)} \sum_{k=1}^{N_{exp}} \omega_k U_{hist,k}(t_j) \right) \\ &= \frac{1}{\Gamma(1-\gamma)} \left[\sum_{k=1}^{N_{exp}} \int_0^{t_{j-2}} \omega_k e^{-\tilde{s}_k(t_{j-1}+\tau-s)} u'(s) ds + \sum_{k=1}^{N_{exp}} \int_{t_{j-2}}^{t_{j-1}} \omega_k e^{-\tilde{s}_k(t_j-s)} u'(s) ds \right] \\ &= \frac{1}{\Gamma(1-\gamma)} \sum_{k=1}^{N_{exp}} \omega_k \left[e^{-\tilde{s}_k\tau} U_{hist,k}(t_{j-1}) + \int_{t_{j-2}}^{t_{j-1}} e^{-\tilde{s}_k(t_j-s)} u'(s) ds \right], \end{aligned} \quad (\text{A.2})$$

where $\tilde{s}_k = s_k + b$. To evaluate $U_{hist,k}(t_j)$ for $j = 1, 2, \dots, N_{exp}$, it observes the following simple recurrence relation:

$$\begin{aligned} U_{hist,k}(t_j) &= e^{-\tilde{s}_k\tau} U_{hist,k}(t_{j-1}) + \int_{t_{j-2}}^{t_{j-1}} e^{-\tilde{s}_k(t_j-s)} u'(s) ds \\ &\approx e^{-\tilde{s}_k\tau} U_{hist,k}(t_{j-1}) + \frac{u(t_{j-1}) - u(t_{j-2})}{\tau} \int_{t_{j-2}}^{t_{j-1}} e^{-\tilde{s}_k(t_j-s)} ds \\ &= e^{-\tilde{s}_k\tau} U_{hist,k}(t_{j-1}) + \frac{[u(t_{j-1}) - u(t_{j-2})](1 - e^{-\tilde{s}_k\tau})}{\tau \tilde{s}_k e^{\tilde{s}_k\tau}}. \end{aligned} \quad (\text{A.3})$$

Noting that $U_{hist,k}(t_1) \equiv 0$ when $n = 1$, we have

$${}^F C \mathbb{D}_t^{\gamma, \lambda(t)} u^1 = \frac{u(t_1) - u(t_0)}{\tau\Gamma(2-\gamma)} \left(e^{-b\tau} \tau^{1-\gamma} + b \int_0^\tau e^{-b\theta} \theta^{1-\gamma} d\theta \right),$$

where we define

$${}^F C \mathbb{D}_t^{\gamma, \lambda(t)} u^j = \frac{u(t_j) - u(t_{j-1})}{\tau\Gamma(2-\gamma)} \left(e^{-b\tau} \tau^{1-\gamma} + b \int_0^\tau e^{-b\theta} \theta^{1-\gamma} d\theta \right) + \frac{1}{\Gamma(1-\gamma)} \sum_{k=1}^{N_{exp}} \omega_k U_{hist,k}(t_j) \quad (\text{A.4})$$

as the approximate discrete operator for evaluating ${}_0^C D_t^{\gamma, \lambda(t)} u(t) |_{t=t_j}$ quickly and $U_{hist,k}(t_j)$ can be computed via Eq. (A.3). At each time step, it remarked that we only need $\mathcal{O}(1)$ work to compute $U_{hist,k}(t_j)$ since $U_{hist,k}(t_{j-1})$ is known at that point. Thus, the total work is reduced from $\mathcal{O}(M^2)$ to $\mathcal{O}(MN_{exp})$, and the total memory requirement is reduced from $\mathcal{O}(M)$ to $\mathcal{O}(N_{exp})^2$.

Similar to [47], replacing the $L1$ -type approximation (cf. Lemma 2.1) for the generalized Caputo fractional derivative by our fast evaluation scheme ${}_0^{FC} \mathbb{D}_t^{\gamma, \lambda(t)}$, we obtain a novel implicit difference scheme of the following form

$$\begin{cases} {}_0^{FC} \mathbb{D}_t^{\gamma, \lambda(t)} u_i^{j+1} = \xi_i^{j+1} (\delta_h^\alpha u_i^{j+1}) + f_i^{j+1}, & i = 1, 2, \dots, N-1, \quad j = 0, 1, \dots, M-1, \\ u_i^0 = \phi(x_i), & i = 0, 1, \dots, N, \\ u_0^{j+1} = \varphi(t_{j+1}), \quad u_N^{j+1} = \psi(t_{j+1}), & j = 0, 1, \dots, M-1, \end{cases} \quad (\text{A.5})$$

which nearly reaches the approximation order of $\mathcal{O}(\tau^{2-\gamma} + h^2)$; see numerical results in the next context. At each time step t_{j+1} , evaluating the right hand side (i.e., the known solutions in the previous time levels) and inverting the linear system have $\mathcal{O}(NN_{exp})$ and $\mathcal{O}(I_{avg}N \log N)$ computational complexity, respectively, which leads to an overall computational complexity of $\mathcal{O}(MN(N_{exp} + I_{avg} \log N))$, where $I_{avg} (\ll N)$ is the average number of iterations required for solving the resultant linear system in each time step. By contrast, if we use the Gaussian elimination to solve the resultant linear systems of Eq. (3.3), the overall computational complexity of the implicit difference scheme (2.3) is about $\mathcal{O}(MN^3 + M^2N)$ operations.

Example A.1 In this example, we test the fast difference scheme (A.5) and direct difference scheme (2.3) for solving the same model problem in **Example 2** except different diffusion coefficient $\xi(x, t) = 10(1/2 + x^2 + \sin t)$. Let $\epsilon = 10^{-9}$ for the fast difference scheme (A.5) and Tables A.9-A.10 are reported to evaluate the accuracy and efficiency of the algorithms proposed.

Tables A.9–A.10 illustrate the temporal/spatial errors, convergence orders and CPU time of the methods. It can be seen clearly from Table A.9 that when $\tau = 2^{-11}$, both “Error_∞” and “Error₂” of two implicit difference schemes for the variable coefficient GTSFDEs with different (γ, α, b) ’s decreases steadily for smaller h , and the order of accuracy in time is about two. Fixing $N = \lceil 2M^{(2-\gamma)/2} \rceil$, Table A.10 lists the maximum-norm and L_2 -norm errors and illustrates that the spatial convergence order is of $\tau^{2-\gamma}$. In conclusion, Tables A.9–A.10 confirm that the rate of the truncation error of two IDS schemes (2.3) and (A.5) is $\mathcal{O}(\tau^{2-\gamma} + h^2)$. However, it seems that the temporal errors of fast scheme (A.5) change slightly irregularly compared to those of the direct scheme (2.3), especially for the case of (0.2, 1.1, 2.0). Moreover, the fast scheme (A.5) requires less CPU time than the direct scheme (2.3) for the variable-coefficient GTSFDEs with different (γ, α, b) ’s. In conclusion, although the derived fast scheme (A.5)³ needs less CPU time and memory cost than the direct scheme (2.3), further analysis is still required to assess its stability and convergence properties.

Acknowledgments

The authors are grateful to Prof. Jiwei Zhang and Dr. Hong-Lin Liao for their constructive discussions and insightful comments. This research is supported by NSFC (11801463 and 61772003), the Fundamental Research Funds for the Central Universities (JBK1902028) and the Ministry of Education of Humanities and Social Science Layout Project (19JYA790094).

References

²In our experiments, it always finds that $N_{exp} < 70$.

³In fact, the above fast scheme can easily utilize the non-uniform temporal steps [53, 54], which can enhance the (numerical) temporal convergence order of difference schemes for the variable-coefficient GTSFDEs (even with the weak singularity at initial time). The corresponding test codes are available by authors’ emails.

Table A.9: L_2 -norm and maximum norm errors versus grid size reduction when $\tau = 2^{-11}$ and $p = 0.7$ in Example A.1.

(γ, α, b)	N	Direct scheme (2.3)					Fast scheme (A.5)				
		Error $_{\infty}$	Rate $_{\infty}$	Error $_2$	Rate $_2$	CPU(s)	Error $_{\infty}$	Rate $_{\infty}$	Error $_2$	Rate $_2$	CPU(s)
(0.2,1.1,1.0)	10	7.3589e-2	—	7.0444e-2	—	3.578	7.3581e-2	—	7.0438e-2	—	0.335
	20	1.7410e-2	2.0796	1.7101e-2	2.0424	3.913	1.7404e-2	2.0799	1.7095e-2	2.0428	0.408
	40	4.1567e-3	2.0664	4.1035e-3	2.0592	4.159	4.1515e-3	2.0677	4.0983e-3	2.0605	0.469
	80	1.1354e-3	1.8722	9.8777e-4	2.0546	5.910	1.1443e-3	1.8592	9.8257e-4	2.0604	1.157
(0.5,1.5,1.0)	10	4.8279e-2	—	4.6207e-2	—	3.586	4.8274e-2	—	4.6202e-2	—	0.343
	20	1.1381e-2	2.0848	1.0791e-2	2.0983	3.967	1.1377e-2	2.0851	1.0787e-2	2.0987	0.417
	40	2.7033e-3	2.0738	2.5503e-3	2.0811	4.278	2.6990e-3	2.0756	2.5463e-3	2.0828	0.482
	80	6.7243e-4	2.0073	6.0900e-4	2.0662	5.935	6.7315e-4	2.0034	6.0516e-4	2.0730	1.161
(0.9,1.9,1.0)	10	4.6595e-2	—	4.6972e-2	—	3.584	4.6593e-2	—	4.6969e-2	—	0.328
	20	1.1365e-2	2.0356	1.1402e-2	2.0425	3.966	1.1363e-2	2.0358	1.1400e-2	2.0427	0.396
	40	2.7816e-3	2.0306	2.7753e-3	2.0386	4.197	2.7797e-3	2.0313	2.7734e-3	2.0393	0.473
	80	6.8243e-4	2.0272	6.7697e-4	2.0355	5.857	6.8051e-4	2.0302	6.7506e-4	2.0386	1.149
(0.2,1.1,2.0)	10	6.9685e-2	—	6.6419e-2	—	3.285	6.9679e-2	—	6.6415e-2	—	0.324
	20	1.6438e-2	2.0838	1.6132e-2	2.0417	3.652	1.6434e-2	2.0840	1.6128e-2	2.0419	0.373
	40	3.9206e-3	2.0679	3.8721e-3	2.0587	3.983	3.9167e-3	2.0690	3.8682e-3	2.0598	0.461
	80	1.0747e-3	1.8671	9.3218e-4	2.0544	5.597	1.0747e-3	1.8657	9.2820e-4	2.0592	1.112
(0.5,1.5,2.0)	10	4.5268e-2	—	4.3322e-2	—	3.265	4.5265e-2	—	4.3318e-2	—	0.321
	20	1.0665e-2	2.0856	1.0114e-2	2.0987	3.512	1.0662e-2	2.0859	1.0110e-2	2.0992	0.369
	40	2.5332e-3	2.0739	2.3895e-3	2.0816	3.898	2.5300e-3	2.0753	2.3865e-3	2.0828	0.458
	80	6.2593e-4	2.0169	5.7014e-4	2.0673	5.697	6.2648e-4	2.0138	5.6752e-4	2.0722	1.116
(0.9,1.9,2.0)	10	4.3556e-2	—	4.3908e-2	—	3.298	4.3554e-2	—	4.3906e-2	—	0.319
	20	1.0623e-2	2.0357	1.0657e-2	2.0427	3.557	1.0621e-2	2.0359	1.0656e-2	2.0428	0.372
	40	2.5992e-3	2.0311	2.5935e-3	2.0388	3.935	2.5978e-3	2.0316	2.5921e-3	2.0395	0.463
	80	6.3724e-4	2.0282	6.3217e-4	2.0365	5.713	6.3580e-4	2.0306	6.3074e-4	2.0390	1.126

Table A.10: L_2 -norm, maximum norm errors and CPU time (in seconds) versus grid size reduction when $N = \lceil 2M^{(2-\gamma)/2} \rceil$ and $p = 0.7$ in Example A.1.

(γ, α, b)	M	Direct scheme (2.3)					Fast scheme (A.5)				
		Error $_{\infty}$	Rate $_{\infty}$	Error $_2$	Rate $_2$	CPU(s)	Error $_{\infty}$	Rate $_{\infty}$	Error $_2$	Rate $_2$	CPU(s)
(0.2,1.1,1.0)	2^5	3.2759e-3	–	3.2241e-3	–	0.008	3.7666e-3	–	2.9594e-3	–	0.007
	2^6	1.0351e-3	1.6621	8.9483e-4	1.8492	0.029	1.2961e-3	1.5391	7.6594e-4	1.9500	0.031
	2^7	3.1910e-4	1.6977	2.4837e-4	1.8491	0.264	4.4060e-4	1.5566	2.0299e-4	1.9158	0.254
	2^8	9.5866e-5	1.7349	6.8823e-5	1.8515	2.873	1.5160e-4	1.5392	5.8937e-5	1.7842	2.859
(0.5,1.5,1.0)	2^6	2.1236e-3	–	2.0025e-3	–	0.012	2.0134e-3	–	1.9017e-3	–	0.013
	2^7	7.4051e-4	1.5199	6.7840e-4	1.5616	0.052	7.5084e-4	1.4231	6.2573e-4	1.6037	0.053
	2^8	2.7349e-4	1.4370	2.3228e-4	1.5463	0.356	2.7741e-4	1.4365	2.0565e-4	1.6053	0.334
	2^9	9.9638e-5	1.4567	8.0300e-5	1.5324	2.703	1.0111e-4	1.4561	6.7254e-5	1.6125	2.442
(0.9,1.9,1.0)	2^7	5.7500e-3	–	5.7539e-3	–	0.019	5.7304e-3	–	5.7345e-3	–	0.021
	2^8	2.5255e-3	1.1870	2.5185e-3	1.1920	0.078	2.5143e-3	1.1885	2.5073e-3	1.1935	0.054
	2^9	1.1846e-3	1.0922	1.1776e-3	1.0967	0.303	1.1782e-3	1.0936	1.1713e-3	1.0980	0.161
	2^{10}	5.3828e-4	1.1380	5.3354e-4	1.1422	1.776	5.3475e-4	1.1396	5.3004e-4	1.1439	0.705
(0.2,1.1,2.0)	2^5	3.1058e-3	–	3.0395e-3	–	0.007	3.3736e-3	–	2.8288e-3	–	0.008
	2^6	9.7378e-4	1.6733	8.4355e-4	1.8493	0.028	1.1535e-3	1.5483	7.4229e-4	1.9301	0.032
	2^7	2.9435e-4	1.7261	2.3410e-4	1.8493	0.261	3.8784e-4	1.5725	2.0336e-4	1.8679	0.255
	2^8	8.8505e-5	1.7337	6.4856e-5	1.8518	2.901	1.3145e-4	1.5609	5.5811e-5	1.8654	2.861
(0.5,1.5,2.0)	2^6	1.9855e-3	–	1.8722e-3	–	0.011	1.9019e-3	–	1.7954e-3	–	0.012
	2^7	6.8955e-4	1.5258	6.3406e-4	1.5620	0.053	6.9740e-4	1.4474	5.9410e-4	1.5955	0.054
	2^8	2.5469e-4	1.4369	2.1704e-4	1.5467	0.360	2.5766e-4	1.4365	1.9681e-4	1.5939	0.255
	2^9	9.2793e-5	1.4567	7.5014e-5	1.5327	2.699	9.3904e-5	1.4562	6.6809e-5	1.5587	2.434
(0.9,1.9,2.0)	2^7	5.3618e-3	–	5.3656e-3	–	0.020	5.3470e-3	–	5.3510e-3	–	0.021
	2^8	2.3546e-3	1.1872	2.3482e-3	1.1922	0.077	2.3462e-3	1.1884	2.3398e-3	1.1934	0.055
	2^9	1.1044e-3	1.0922	1.0980e-3	1.0967	0.302	1.0996e-3	1.0933	1.0933e-3	1.0977	0.255
	2^{10}	5.0182e-4	1.1380	4.9742e-4	1.1423	1.769	4.9917e-4	1.1394	4.9480e-4	1.1438	0.694

References

- [1] I. Podlubny, *Fractional Differential Equations*, vol. 198 of Mathematics in Science, Academic Press Inc., San Diego, CA (1999).
- [2] S.G. Samko, A.A. Kilbas, O.I. Marichev, *Fractional Integrals and Derivatives: Theory and Applications*, Gordon and Breach Science Publishers, Yverdonn, Switzerland (1993).
- [3] A.A. Kilbas, H.M. Srivastava, J.J. Trujillo, *Theory and Applications of Fractional Differential Equations*, Elsevier, Amsterdam, Netherlands (2006).
- [4] R. Metzler, J. Klafter, The random walk's guide to anomalous diffusion: A fractional dynamics approach, *Phys. Rep.*, 339(1) (2000), pp. 1-77.
- [5] X. Wu, W. Deng, E. Barkai, Tempered fractional Feynman-Kac equation: Theory and examples, *Phys. Rev. E*, 93(3) (2016), Article No. 032151, 15 pages. DOI: 10.1103/PhysRevE.93.032151.
- [6] M.A.F. Santos, Mittag-Leffler memory kernel in Lévy flights, *Mathematics*, 7(9) (2019), Article No. 766, 13 pages. DOI: 10.3390/math7090766.
- [7] T. Sandev, A. Chechkin, H. Kantz, R. Metzler, Diffusion and Fokker-Planck-Smoluchowski equations with generalized memory kernel, *Fract. Calc. Appl. Anal.*, 18(4) (2015), pp. 1006-1038.
- [8] A.A. Alikhanov, A time-fractional diffusion equation with generalized memory kernel in differential and difference settings with smooth solutions, *Comput. Methods Appl. Math.*, 17(4) (2017), pp. 647-660.
- [9] Z. Zhang, W. Deng, Numerical approaches to the functional distribution of anomalous diffusion with both traps and flights, *Adv. Comput. Math.*, 43(4) (2017), pp. 699-732.
- [10] E. Hanert, C. Piret, A Chebyshev pseudospectral method to solve the space-time tempered fractional diffusion equation, *SIAM J. Sci. Comput.*, 36(4) (2014), pp. A1797-A1812.
- [11] F. Sabzikar, M. M. Meerschaert, J. Chen, Tempered fractional calculus, *J. Comput. Phys.*, 293 (2015), pp. 14-28.
- [12] L. Guo, F. Zeng, I. Turner, K. Burrage, G.E. Karniadakis, Efficient multistep methods for tempered fractional calculus: Algorithms and simulations, *SIAM J. Sci. Comput.*, 41(4) (2019), pp. A2510-A2535.
- [13] M. Chen, W. Deng, High order algorithm for the time-tempered fractional Feynman-Kac equation, *J. Sci. Comput.*, 76(2) (2018), pp. 867-887.
- [14] G.-H. Gao, A.A. Alikhanov, Z.-Z. Sun, The temporal second order difference schemes based on the interpolation approximation for solving the time multi-term and distributed-order fractional sub-diffusion equations, *J. Sci. Comput.*, 73(1) (2017), pp. 93-121.
- [15] Y. Xu, Z. He, O.P. Agrawal, Numerical and analytical solutions of new generalized fractional diffusion equation, *Comput. Math. Appl.*, 66(10) (2013), pp. 2019-2029.
- [16] G. Chi, G. Li, C. Sun, X. Jia, Numerical solution to the space-time fractional diffusion equation and inversion for the space-dependent diffusion coefficient, *J. Comput. Theor. Trans.*, 46(2) (2017), pp. 122-146.
- [17] M.L. Morgado, M. Rebelo, Well-posedness and numerical approximation of tempered fractional terminal value problems, *Fract. Calc. Appl. Anal.*, 20(5) (2017), pp. 1239-1262.
- [18] W. Deng, B. Li, W. Tian, Pi. Zhang, Boundary problems for the fractional and tempered fractional operators, *Multiscale Model. Simul.*, 16(1) (2018), pp. 125-149.
- [19] W. Deng, Z. Zhang, *High Accuracy Algorithms for the Differential Equations Governing Anomalous Diffusion: Algorithm and Models for Anomalous Diffusion*, World Scientific Publishing, Singapore (2019).
- [20] M. M. Meerschaert, Help about your paper 'Tempered fractional calculus': The fundamental solution of the tempered fractional advection-diffusion equations (with X.-M. Gu), *Personal Communication*, July 6, 2018.
- [21] C. Tadjeran, M.M. Meerschaert, H.-P. Scheffler, A second-order accurate numerical approximation for the fractional diffusion equation, *J. Comput. Phys.*, 213(1) (2006), pp. 205-213.
- [22] M.M. Meerschaert, C. Tadjeran, Finite difference approximations for two-sided space-fractional partial differential equations, *Appl. Numer. Math.*, 56(1) (2006), pp. 80-90.
- [23] F.-R. Lin, S.-W. Yang, X.-Q. Jin, Preconditioned iterative methods for fractional diffusion equation, *J. Comput. Phys.*, 256 (2014), pp. 109-117.
- [24] E. Sousa, C. Li, A weighted finite difference method for the fractional diffusion equation based on the Riemann-Liouville derivative, *Appl. Numer. Math.*, 90 (2015), pp. 22-37.
- [25] X.-L. Lin, M.K. Ng, H.-W. Sun, Stability and convergence analysis of finite difference schemes for time-dependent space-fractional diffusion equations with variable diffusion coefficients, *J. Sci. Comput.*, 75(2) (2018), pp. 1102-1127.
- [26] X. Zheng, V.J. Ervin, H. Wang, Spectral approximation of a variable coefficient fractional diffusion equation in one space dimension, *Appl. Math. Comput.*, 361 (2019), pp. 98-111.
- [27] W. Qu, S.-L. Lei, S.-W. Vong, A note on the stability of a second order finite difference scheme for space fractional diffusion equations, *Numer. Algebra Contr. Optim.*, 4(4) (2014), pp. 317-325.
- [28] F.-R. Lin, W.-D. Liu, The accuracy and stability of CN-WSGD schemes for space fractional diffusion equation, *J. Comput. Appl. Math.*, 363 (2020), pp. 77-91.
- [29] S. Vong, P. Lyu, On a second order scheme for space fractional diffusion equations with variable coefficients, *Appl. Numer. Math.*, 137 (2019), pp. 34-48.
- [30] L. Feng, P. Zhuang, F. Liu, I. Turner, Q. Yang, Second-order approximation for the space fractional diffusion equation with variable coefficient, *Progr. Fract. Differ. Appl.*, 1(1) (2015), pp. 23-35.
- [31] X.-L. Lin, P. Lyu, M.K. Ng, H.-W. Sun, S. Vong, An efficient second-order convergent scheme for one-side space fractional diffusion equations with variable coefficients, submitted to *Commun. Appl. Math. Comput.*, arXiv preprint, arXiv:1902.08363, 22 Feb. 2019, 28 pages.

- [32] X.-L. Lin, M.K. Ng, H.-W. Sun, Efficient preconditioner of one-sided space fractional diffusion equation, *BIT*, 58(3) (2018), pp. 729-748.
- [33] F. Liu, P. Zhuang, I. Turner, K. Burrage, V. Anh, A new fractional finite volume method for solving the fractional diffusion equation, *Appl. Math. Model.*, 38(15-16) (2014), pp. 3871-3878.
- [34] R.-F. Ren, H.-B. Li, W. Jiang, M.-Y. Song, An efficient Chebyshev-tau method for solving the space fractional diffusion equations, *Appl. Math. Comput.*, 224 (2013), pp. 259-267.
- [35] J. Ma, J. Liu, Z. Zhou, Convergence analysis of moving finite element methods for space fractional differential equations, *J. Comput. Appl. Math.*, 255 (2014), pp. 661-670.
- [36] E.H. Doha, A.H. Bhrawy, S.S. Ezz-Eldien, Numerical approximations for fractional diffusion equations via a Chebyshev spectral-tau method, *Cent. Eur. J. Phys.*, 11(10) (2013), pp. 1494-1503.
- [37] X. Ji, H. Tang, High-order accurate Runge-Kutta (local) discontinuous Galerkin methods for one- and two-dimensional fractional diffusion equations, *Numer. Math. Theor. Meth. Appl.*, 5(3) (2012), pp. 333-358.
- [38] L.B. Feng, P. Zhuang, F. Liu, I. Turner, Stability and convergence of a new finite volume method for a two-sided space-fractional diffusion equation, *Appl. Math. Comput.*, 257 (2015), pp. 52-65.
- [39] J. Liu, H. Fu, H. Wang, X. Chai, A preconditioned fast quadratic spline collocation method for two-sided space-fractional partial differential equations, *J. Comput. Appl. Math.*, 360 (2019), pp. 138-156.
- [40] J. Pan, M.K. Ng, H. Wang, Fast iterative solvers for linear systems arising from time-dependent space-fractional diffusion equations, *SIAM J. Sci. Comput.*, 38(5) (2016), pp. A2806-A2826.
- [41] Z.-P. Hao, Z.-Z. Sun, W.-R. Cao, A fourth-order approximation of fractional derivatives with its applications, *J. Comput. Phys.*, 281 (2015), pp. 787-805.
- [42] A.Kh. Khibiev, Stability and convergence of difference schemes for the multi-term time-fractional diffusion equation with generalized memory kernels, *J. Samara State Tech. Univ., Ser. Phys. Math. Sci.*, in press, 23(3) (2019), pp. 1-16. DOI: 10.14498/vsgtu1690. (in Russian)
- [43] H. Fu, H. Wang, A preconditioned fast parareal finite difference method for space-time fractional partial differential equation, *J. Sci. Comput.*, 78(3) (2019), pp. 1724-1743.
- [44] M.A. Firoozjaee, S.A. Yousefi, H. Jafari, A numerical approach to Fokker-Planck equation with space- and time-fractional and non fractional derivatives, *Commun. Math. Comput. Chem.*, 74(3) (2015), pp. 449-464.
- [45] X.-L. Lin, M.K. Ng, A fast solver for multidimensional time-space fractional diffusion equation with variable coefficients, *Comput. Math. Appl.*, 78(5) (2019), pp. 1477-1489.
- [46] Z. Zhao, X.-Q. Jin, M.M. Lin, Preconditioned iterative methods for space-time fractional advection-diffusion equations, *J. Comput. Phys.*, 319 (2016), pp. 266-279.
- [47] S. Jiang, J. Zhang, Q. Zhang, Z. Zhang, Fast evaluation of the Caputo fractional derivative and its applications to fractional diffusion equations, *Commun. Comput. Phys.*, 21(3) (2017), pp. 650-678.
- [48] S.-L. Lei, H.-W. Sun, A circulant preconditioner for fractional diffusion equations, *J. Comput. Phys.*, 242 (2013), pp. 715-725.
- [49] S. Vong, P. Lyu, X. Chen, S.-L. Lei, High order finite difference method for time-space fractional differential equations with Caputo and Riemann-Liouville derivatives, *Numer. Algorithms*, 72(1) (2016), pp. 195-210.
- [50] X.-M. Gu, T.-Z. Huang, C.-C. Ji, B. Carpentieri, A.A. Alikhanov, Fast iterative method with a second-order implicit difference scheme for time-space fractional convection-diffusion equation, *J. Sci. Comput.*, 72(3) (2017), pp. 957-985.
- [51] B. Jin, R. Lazarov, Z. Zhou, An analysis of the L_1 scheme for the subdiffusion equation with nonsmooth data, *IMA J. Numer. Anal.*, 36(1) (2016), pp. 197-221.
- [52] B. Jin, R. Lazarov, Z. Zhou, Numerical methods for time-fractional evolution equations with nonsmooth data: A concise overview, *Comput. Meth. Appl. Mech. Eng.*, 346 (2019), pp. 332-358.
- [53] M. Stynes, E. O'Riordan, J.L. Gracia, Error analysis of a finite difference method on graded meshes for a time-fractional diffusion equation, *SIAM J. Numer. Anal.*, 55(2) (2017), pp. 1057-1079.
- [54] H.-L. Liao, D. Li, J. Zhang, Sharp error estimate of the nonuniform L_1 formula for linear reaction-subdiffusion equations, *SIAM J. Numer. Anal.*, 56(2) (2018), pp. 1112-1133.
- [55] M.K. Ng, *Iterative Methods for Toeplitz Systems*, Oxford University Press, New York, NY (2004).
- [56] M. Donatelli, M. Mazza, S. Serra-Capizzano, Spectral analysis and structure preserving preconditioners for fractional diffusion equations, *J. Comput. Phys.*, 307 (2016), pp. 262-279.
- [57] J. Pan, R. Ke, M.K. Ng, H.-W. Sun, Preconditioning techniques for diagonal-times-Toeplitz matrices in fractional diffusion equations, *SIAM J. Sci. Comput.*, 36(6) (2014), pp. A2698-A2719.
- [58] I. Gohberg, V. Olshevsky, Circulants, displacements and decompositions of matrices, *Integr. Equ. Oper. Theory*, 15(5) (1992), pp. 730-743.
- [59] Y.-L. Zhao, P.-Y. Zhu, X.-M. Gu, X.-L. Zhao, J. Cao, A limited-memory block bi-diagonal Toeplitz preconditioner for block lower triangular Toeplitz system from time-space fractional diffusion equation, *J. Comput. Appl. Math.*, 362 (2019), pp. 99-115.
- [60] Y.-C. Huang, S.-L. Lei, A fast numerical method for block lower triangular Toeplitz with dense Toeplitz blocks system with applications to time-space fractional diffusion equations, *Numer. Algorithms*, 76(3) (2017), pp. 605-616.
- [61] M. Li, X.-M. Gu, C. Huang, M. Fei, G. Zhang, A fast linearized conservative finite element method for the strongly coupled nonlinear fractional Schrödinger equations, *J. Comput. Phys.*, 358 (2018), pp. 256-282.
- [62] H.A. van der Vorst, Bi-CGSTAB: A fast and smoothly converging variant of Bi-CG for the solution of nonsymmetric linear systems, *SIAM J. Sci. Stat. Comput.* 13(2) (1992), pp. 631-644.